Universiteit Utrecht

Faculteit Bètawetenschappen

Efficient filtration system inspired by the kidney:
3D modeling of an active osmotic exchanger in COMSOL

Bachelor Thesis

Johan Verheij

Natuur- en Sterrenkunde

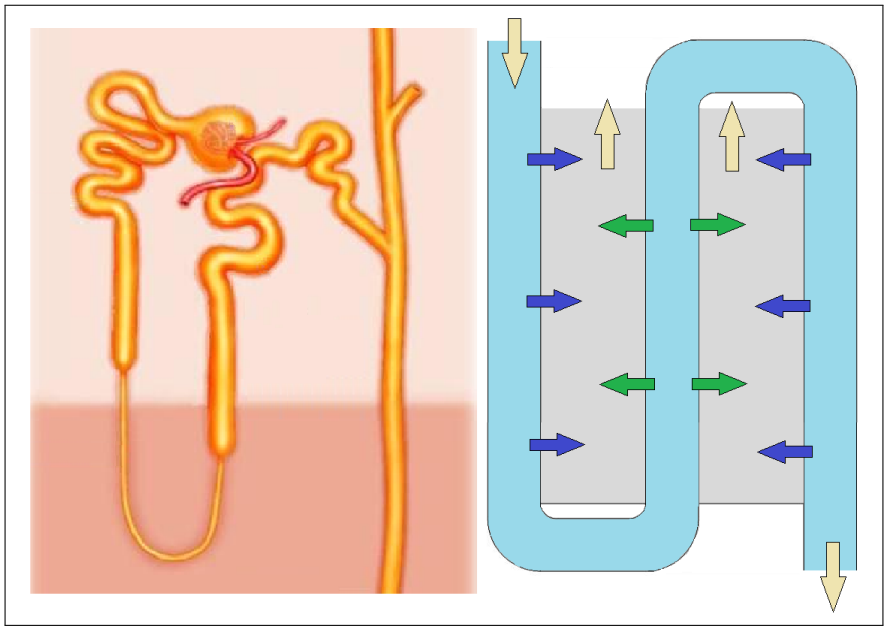

Supervisors:

Prof. Dr. René van Roij
Institute for Theoretical Physics

Ben Werkhoven MSc
Institute for Theoretical Physics

Dr. Joost de Graaf
Institute for Theoretical Physics

June 13, 2018

Abstract

Nowadays, recycling of water in an (energy) efficient way is a challenge that needs to be engaged. This thesis provides a theoretical framework that can be used to build a physical model of a filtration device. Additionally we developed some building blocks in COMSOL that can be used to build a numerical model for such a device, based on the human kidney. Inspiration from the kidney is used because this is one of the most efficient filtration devices. In our model we find that the ion concentration profiles are consistent with the findings of Marbach and Bocquet [Phys. Rev. X **3**, 031008 (2016)] . Based on this thesis one could build a more complete model of a filtration device. Such a model could be used to build a filtration device for small-scale water recycling or maybe even an artificial kidney.

Front page: Figure on the left is an overview of the human nephron, figure taken and edited from: `https://socratic.org/questions/5708bab211ef6b107dd76e34`. Figure on the right side is a schematic overview of the model we tried to build. Yellow arrows indicate a flow of the fluid and solutes, blue arrows a flow of fluid and green arrows a flow of ions.

Contents

1 Introduction

Techniques used in the process of water recycling and filtration nowadays are based on reverse osmosis and the use of semi-permeable membranes [1]. For reverse osmosis a (high) pressure gradient is applied to a solution and as a result of this parts of the solution flows through a selective membrane, leaving behind the unwanted substances. The high pressure required and the need for selectivity is a challenge in building efficient filtration devices. It is also costly in terms of the energy needed for this process. State-of-the-art seawater desalination plants that use reverse osmosis, consume 4-14 kJ for the production of one liter of fresh water [1, 2]. There are recent developments in the field of nanoscale materials, e.g. the use of graphene, nanotubes or advanced membranes [3–5]. These new materials and new techniques are promising in terms of efficiecy. However, more steps need to be taken for making progress in this field.
In the paper *Active Osmotic Exchanger for Efficient Nanofiltration Inspired by the Kidney*, Marbach and Bocquet argue that a necessary step to boost the efficiency of the separation processes requires out-of-the-box ideas. They come up with the idea to mimic the process of filtration in the kidney. Biological processes are able to fulfill the task of efficient filtration at low energy cost. From calculations in [6] it follows that the thermodynamical limit in the human kidney is ~ 0.2 kJ per liter of filtered blood. The calculation is based on some assumptions, so this value is not determined exactly. But the important thing is that this value is close to the real energy consumption in the human kidney of 0.5 kJ/L [7]. Standard dialytic filtration systems, however, require 2 orders of magnitude more energy. For example the hemodialysis system of [8] uses at least $\sim$ 200kJ/L to perform the filtration.
Per day, 200 L of water and 1.5 kg of salt are recycled in the human kidney. In this process $\sim 99\%$ of the water is reabsorbed. The kidney consists of about one million substructures, called nephrons, that perform the actual filtration process [7, 9, 10]. One of the key features of the process is the U-shaped loop of Henle in the nephron which acts as an active osmotic exchanger. Due to this geometry the kidney benefits very efficiently from osmotic transport, lowering the energy cost of the filtration process. There are many studies on the nephron from a biological or physiological point of view [11–16]. However, we will study the nephron from a physical perspective.

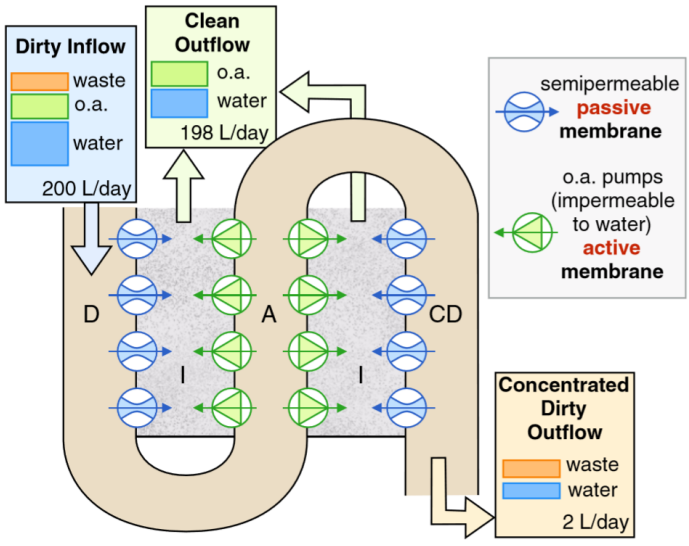

Figure 1: Schematic overview of the geometry used in Marbach's model [17] for the nephron, consisting of 3 different tubules: the descending tube (D) with walls permeable to water, the ascending tube (A) with active ion pumps, and the collecting duct (CD) again with walls permeable to water; and an interstitium (I) surrounding the tubules. Numbers of in- and outflow are realistic for humans, composition of in- and outflow is a simplified version of reality. Figure taken from [17].

Marbach and Bocquet built a 1D model of the kidney and found some important properties of the model, including a typical reabsorption length l_c and bounds for the water loss fraction η [17]. See Fig. 1 for a schematic overview of the model of the nephron. We will try to build a 3D model (actually a 2D-axisymmetric model) using the COMSOL software and study the properties of our model. We expect to find qualitatively similar result for our 3D model as Marbach and Bocquet for their 1D model, but it is of interest to see whether the 3D character will change the picture.
First we will give a description of the kidney and the nephron from a biological perspective. Secondly we will explain the Michaelis-Menten kinetics that are used to described enzymatic processes, in our case the

kinetics of the sodium pumps. Then we will discuss the physical theory that describes the flow of solutions with electrolytes through small channels. After that we describe the model we built using COMSOL to solve the problem numerically and compare our results with the results of Marbach and Bocquet.

2 The kidney

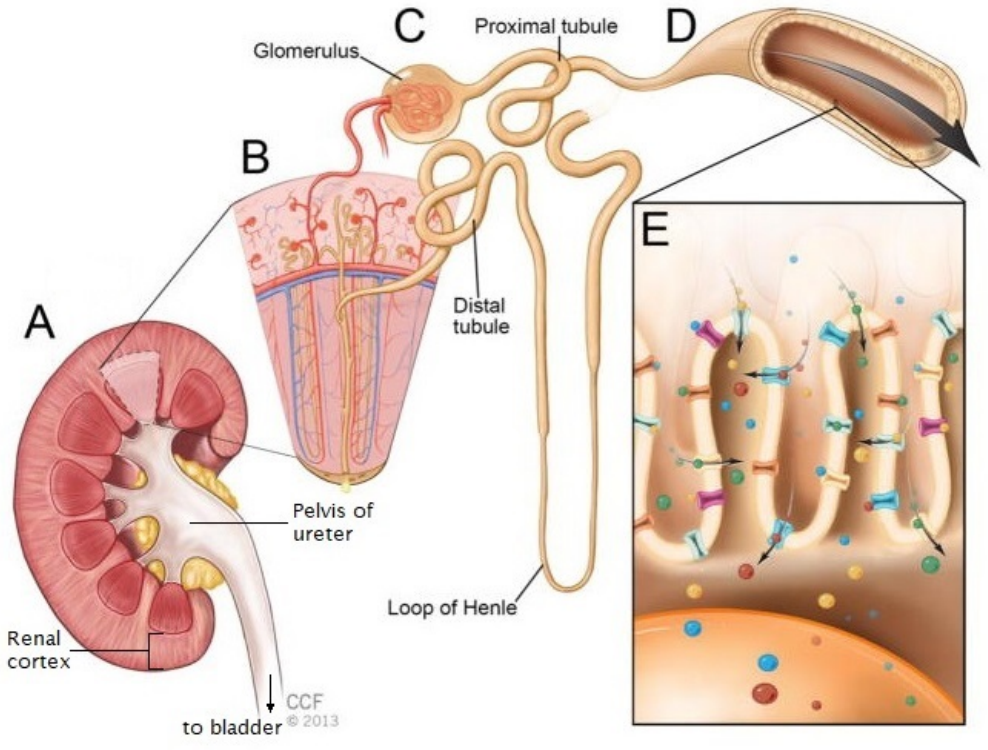

Figure 2: Schematic overview of the kidney. Obtained from [18].

In this section we will discuss the structure and the function of (several parts of) the human kidney. In Fig. 2 a schematic overview is given with the names of relevant constituents.
The kidney is a bean-shaped organ that is approximately 11 cm long in adult humans [19]. The kidney plays an essential role in the homeostasis, i.e. it maintains the stable state of an organism, by filtrating the blood and excreting metabolic waste products (e.g. urea) and regulating several balances (e.g. the water balance). Blood that needs to be filtered enters the kidney via the Renal artery and divides in a lot of small arteries to the renal cortex. In the renal cortex the filtration of the blood starts in the functional units of the kidney. These functional units are called nephrons and each kidney consists of approximately[1] 1 million nephrons [9, 10, 20, 21]. The nephron will be elaborately discussed in section 2.1. The waste, called urine, that is excreted during the filtration process is collected from the nephrons in a collecting duct, which transports the urine to the pelvis of the ureter. The waste leaves the kidney via the ureter to the urinary bladder. The filtrated blood leaves the kidney via the renal vein.
In section 2.1 we largely follow the discussion of Ch. 49-52 of [9] and Ch. 26-28 of [10].

2.1 The Nephron

Each nephron consists of two different parts, the renal corpuscle and the tubular portion. In Fig. 3 an overview of the nephron is shown. In the following sections we will discuss the structure and functions of the renal corpuscle and the tubular part of the nephron.

2.1.1 Structure of the renal corpuscle

The renal corpuscle consists of a glomerulus and the Bowman capsule. The glomerulus is a tuft of small capillaries that is enclosed by the Bowman capsule. Via the afferent arteriole the blood enters the glomerulus

[1] The number of nephrons per kidney can vary widely, by at least tenfold, as can be found in [20].

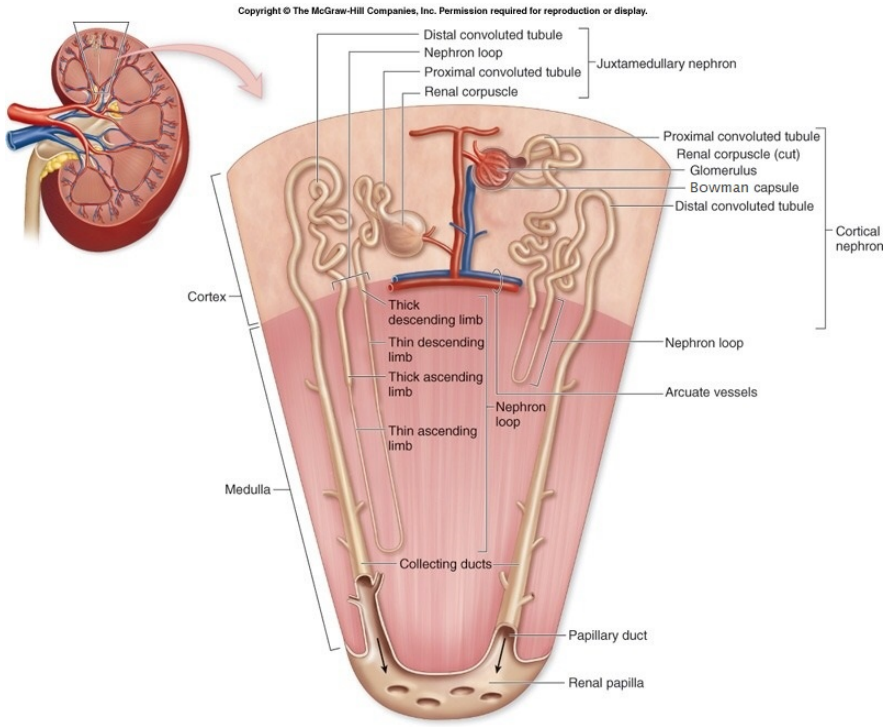

Figure 3: Schematic overview of the nephron. Obtained from: http://platformedical.tumblr.com/post/159403130337

and via the efferent arteriole the filtered blood leaves the glomerulus. The filtrate enters the tubular part of the nephron through the Bowman capsule. Between the glomerular capillaries and the Bowman capsule there is a filtering membrane. This membrane is called the glomerular capillary membrane. It consists of a basement membrane and cells fused on both sides of this membrane. Between those cells small pores exist with a diameter of about 8 nm[10]. In addition the filtering membrane is also negatively charged, making it less permeable to negatively charged ions.

2.1.2 Function of the renal corpuscle

The renal corpuscle performs the first step in the formation of urine. One of the main functions of the glomerulus is to allow the filtration of small solutes and prevent (or at least restrict) the entrance of larger molecules into the nephron. The characteristics of the membrane between the glomerular capillaries and the Bowman capsule ensures that the filtrate contains no cellular elements (e.g. red blood cells) and essentially no proteins (e.g. albumin). These substances are not in the filtrate because of their relatively large size and for proteins also due to the negative charge of the molecules. All other substances are present in the filtrate.[2] The glomerular filtration rate (GFR) and single nephron glomerular filtration rate (SNGFR) are a measure of the total quantity of filtrate formed per unit of time in all nephrons together. The GFR and SNGFR can be calculated as:

$$\mathrm{GFR} = \mathrm{K_f} * p_{net} \qquad or \qquad \mathrm{GFR} = \mathrm{RPF} * \mathrm{F_f} \tag{2.1}$$

$$\mathrm{SNGFR} = \mathrm{SNK_f} * p_{net} \tag{2.2}$$

where $\mathrm{K_f}$ and $\mathrm{SNK_f}$ are the capillary filtration coefficient for both kidneys and for a single nephron, respectively, and $\mathrm{F_f}$ the filtration fraction. The filtration coefficient is the product of the permeability and filtering

[2]Examples of substances that are present in the filtrate under normal conditions are: Na^+, Cl^-, K^+, HCO^-_3, urea, glucose etc.

surface area of the capillaries. RPF is short for renal plasma flow, the total flow in the arteries measured in ml/min. The net filtration pressure p_{net}, is the sum of the different hydrostatic and osmotic pressures in the glomerulus and the Bowman capsule. The net pressure can be calculated as:

$$p_{net} = p_{H,G} - p_{H,B} - p_{O,G} + p_{O,B}, \tag{2.3}$$

where $p_{H,G}$ is the hydrostatic pressure in the glomerulus, $p_{H,B}$ is the hydrostatic pressure in the Bowman capsule, $p_{O,G}$ is the osmotic pressure in the glomerulus and $p_{O,B}$ is the osmotic pressure in the Bowman capsule. Note that the osmotic pressure in the glomerulus opposes the filtration.
A recent study[3] showed that the average GFR of the human kidney is 115 ml/min and the SNGFR is 80 nl/min [21]. Another study reported an average GFR of 104 ml/min [22]. This second study also reported values for other variables, see table 1. For convenience let's assume that GFR = 100 ml/min and the number of nephrons is 1 million, resulting in a SNGFR of 100 nl/min. From the values in table 1 we get that p_{net} = 40 - 24.9 $\approx$ 15 mmHg[4]. Note that $p_{H,G}$ - $p_{H,B}$ = 40 mmHg is an assumption, because this has not been measured directly in humans. In other literature they use 10 mmHg, 11.3-12.5 mmHg and 15-20 mmHg [9–11]. For convenience we will use p_{net} = 10 mmHg. If we use GFR = 100 ml/min and p_{net} = 10 mmHg to calculate the K_f from Eq. (2.1), we get K_f = 100/10 = 10 ml·min^{-1}·mmHg^{-1}. And for the single nephron K_f we get SNK_f = 100/10 = 10 nl·min^{-1}·mmHg^{-1}.

Table 1: Reported values in study [22]

RPF	576 ± 127
Filtration fraction	0.19 ± 0.04
Arterial pressure*	88.8 ± 8
$2\,K_f$**	11.3 ± 4.9
$p_{O,G}$	24.9 ± 2.5

*Arterial pressure and $p_{H,G}$ are not the same. If the blood enters the glomerular capillaries there is a pressure drop and therefore $p_{H,G}$ is lower than the arterial pressure.
**The two-kidney filtration coefficient is determined using $p_{H,G}$ - $p_{H,B}$ = 40 mmHg.

Another important function of the renal corpuscle is the regulation of the GFR. Under extreme conditions or acute disturbances the GFR is influenced by the sympathetic nervous system, hormones and vasoactive substances in the kidney. Under normal conditions and small disturbances the GFR is mostly influenced by the autoregulation system of the kidney. This autoregulation system regulates the renal blood flow by constriction and dilatation of the afferent and efferent arteriole. The macula densa, located in the juxtaglomerular apparatus, consists of cells that are sensitive to the concentration of NaCl (in the distal convoluted tubule). When the GFR increases, the concentration of NaCl in the filtrate also increases. In the distal convoluted tubule the NaCl is determined almost entirely by the tubular flow rate. At low flow rates, the tubular fluid is maximally dilute and Na^+ and Cl^- concentrations are low. When flow increases, these concentrations rise; the physiological range is approximately 25-60 mM [24]. The increase in NaCl concentration causes the macula densa to release adenosine which causes the constriction of the afferent arteriole. The decrease in blood supply, i.e. lower RPF, means a decrease in GFR. This mechanism is also known as the tubuloglomerular feedback mechanism.

2.1.3 Structure of the tubular part

After the filtration of the blood by glomerular capillary membranes in the renal corpuscle the filtrate flows into the tubular part of the nephron. It flows through the successive parts of the tubule in the following order: the proximal tubule, the loop of Henle, the distal convoluted tubule (DCT), the connecting tubule (CNT) and the collecting duct (CD). The proximal tubule consists of the proximal convoluted tubule (PCT) and the proximal straight tubule[5] (PST). The loop of Henle consists of the thin descending segment (LDS), the thin ascending segment (LAS) and the thick ascending segment (TAS).

The proximal tubule is lined by a single layer of cuboidal epithelial cells[6]. These cells have an extensive

[3]This study is performed on 1388 living kidney donors, the official reported values are: mean GFR 115±24 ml/min and SNGFR 80±40nl/min. The average number of nephrons per kidney was calculated to be 860,000±370,00.
[4]mmHg is defined as the pressure generated by a column of 1 mm of mercury. 1 mmHg = 133.322... Pa [23]
[5]Sometimes also calles the thick descending limb, as in Fig. 3.
[6]Epithelium is the tissue formed by epithelial cells and is one of the four primary tissues. One of the primary tasks of this type of cell is the regulation and exchange of molecules.

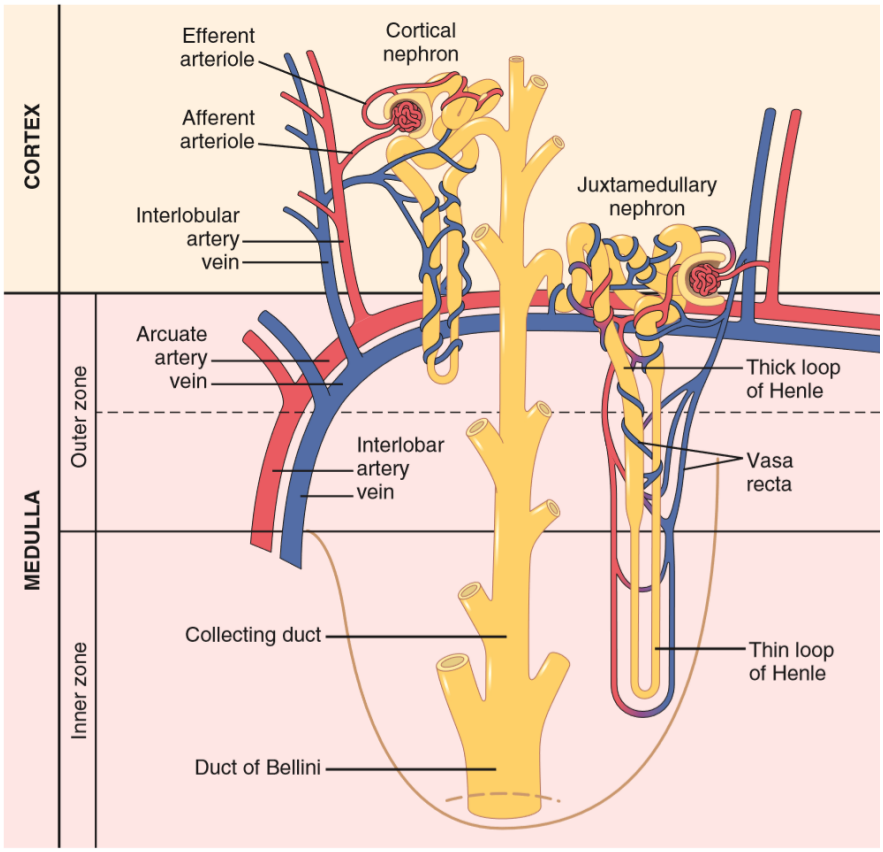

Figure 4: Schematic overview of the two different types of nephrons including the peritubular capillaries. Obtained from [10].

brush border, this enlarges luminal surface area of the cells. The cells also have a large number of mitochondria. A mithochondrion produces adenosine triphosphate (ATP), this is the most important chemical energy carrier that is used in the kidney. This part of the nephron is highly permeable to most substance in the filtrate, including water, and hardly permeable to metabolic waste products.
The loop of Henle consists of three segments. The LDS is highly permeable to water and moderately permeable to most solutes. The LAS is virtually impermeable to water The TAS has cuboidal epithelial cells that are capable of active reabsorption of sodium, chloride and potassium. The thin segments are made of flattened epithelial cells and have a much lower reabsorptive capacity than the thick segment, LDS and LAS do not reabsorb significant amounts of any of the solutes. The TAS is virtually impermeable to water.
The TAS empties into the DCT and has nearly the same properties of TAS. It strongly reabsorbs most of the ions, but it is also virtually impermeable to water.
The CNT and CD have quite similar characteristics, but the are composed of different cell types which have a different functions as will be discussed in the next section. The permeability of this part of the tubular part depends on the concentration of the antidiuretic hormone which will be discussed below.

There are two different types of nephrons: the cortical and juxtamedullary nephrons. The renal corpuscle of the cortical nephrons lies in the outer cortex and the loop of Henle is short, penetrating only a short distance into the medulla. On the contrary, the renal corpuscle of the juxtamedullary nephrons lies deep into the cortex near the medulla. The loop of Henle of this type of nephron is also much longer and reaches deep into the medulla. The functional difference of the two types of nephrons will be discussed in 2.1.4.
The tubular part of the nephron is surrounded by a network of peritubular capillaries. Those peritubular capillaries are a continuation of the efferent arteriole. The peritubular parts of cortical and juxtamedullary nephrons are different. Around the tubules of the cortical nephrons there is an extensive network of per-

itubular capillaries that surrounds the entire tubular part. For the juxtamedullary nephrons, however, the efferent arteriole extends from the glomerulus down into the outer medulla and from there continues as the vasa recta. The vasa recta extends down into the medulla and is different from the 'normal' peritubular capillaries in the fact that they lie parallel to the loop of Henle. The network of peritubular capillaries is less extensive than that of the cortical nephrons. See Fig. 4 for some clarification. The (hydrostatic) pressure in these capillaries is very low $\sim$ 18 mmHg [10]. The functionality of these peritubular capillaries will be discussed in 2.1.4.

We will now give an overview of the typical size of the different segments of the nephron. In table 2 the length and outer diameter of the different parts of the nephron are given. Because the size of the cells on the outside of the tubules the inner diameter is much less than the outer diameter. The size of the epithelial cells is ~ 10 µm. But this size varies for the different portions of the tubules, due to this the inner diameter is fairly constant and $\sim 20 - 30$ µm.

Table 2: Size of different parts of the nephron [9]

Segment	Length (mm)	Outer diameter (μ)
Proximal convoluted tubule	14	55
Thick descending limb	6	55
Thin descending segment, hairpin bend and thin ascending segment	10-15	15
Thick ascending segment	9	30
Distal convoluted tubule	14.5-15	22-50
Collecting duct	20-22	40-200

2.1.4 Function of the tubular part

The function of the tubular part of the nephron is to reabsorb the solutes we need for our body (e.g. sodium, glucose, amino acids) and to excrete the solutes that we have to get rid of (e.g. metabolic waste products). The process of transporting substances from the tubular part of the nephron back to the blood is called tubular reabsorption. If a fluid needs to be reabsorbed it has to be transported through the membranes between the tubules and the interstitial fluid and through to membranes between the interstitial fluid and the peritubular capillaries. Reabsorption of solutes from the tubular part to the interstitium can be done by active or passive transport. Active transport is the movement of molecules against the electrochemical gradient and therefore this form of transport needs energy. The energy is derived from ATP. Substances that are reabsorbed actively include sodium, calcium, glucose and amino acids. This does not mean that all transport of these substances is active, most substances are reabsorbed partially actively and partially passively. Passive transport is the movement of molecules along the electrochemical gradient. This process does not need energy. Substances that are transported passively are chloride and water. This transport mechanisms will be discussed in more detail below.

The transport of substances from the tubular part into the interstitial fluid occurs via two routes: the transcellular route and the paracellular route.

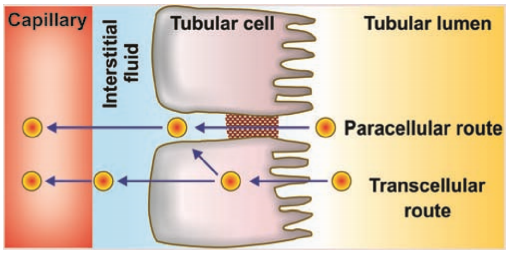

Figure 5: Different routes of transport. Obtained from [9].

We will now discuss the reabsorption of the different substances along the different parts of the nephrons. We will mainly focus on the transport of water, sodium and chloride. In the previous section we discussed the properties of the different tubular parts and now we will explain how this relates to the function of the different parts. For an overview of all the parts of the nephron, see Fig. 6.

The PCT and PST reabsorbs the largest part of the substances due to its special cellular characteristics. About 65 percent of the sodium and water is reabsorbed in the PCT and PST and a slightly lower percentage of the chloride. The most important transport mechanism in this part of the nephron is the sodium-potassium ATPase pump that actively reabsorbs sodium. These pumps are commonly described by Michaelis-Menten kinetics [25, 26]. In section 3 we will give a derivation and discussion on this

kinetics. In the PCT the most essential substances, like glucose and amino acids, are reabsorbed almost completely. The reabsorption of these essential substances is done by the active co-transport with sodium. In the PST the very little of the glucose and amino acids remain, and the sodium is now transported actively mainly with chloride ions. Because of the higher concentration of chloride in the PST than in the PCT, a part of the chloride also ends up in the interstitial fluid by diffusion. Because the active transport of salts into the interstitial fluid the salt concentration in the interstitium increases and water will passively follows by osmosis. The high permeability of the PCT and PST to water ensures that water reabsorption by osmosis keeps pace with the sodium reabsorption. This keeps the osmolarity along the PCT and PST virtually constant.

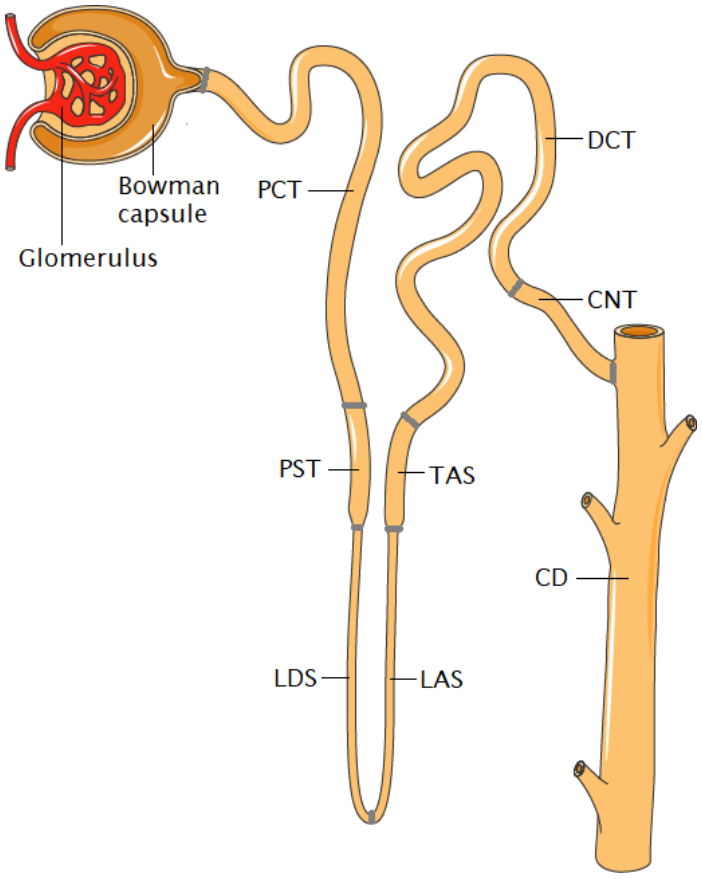

Figure 6: Overview of the names of the different parts of the nephron as described in Sec. 2.1.3.

After the proximal tubule the fluid enters the loop of Henle. The function of the LDS is allowing substances to diffuse through its walls. Because of the high permeability to water, mainly water is reabsorbed by osmosis. About 20 percent of the water is reabsorbed in this part of the nephron. The LAS and TAS are impermeably to water and no therefore (almost) no reabsorption of water occurs. In the TAS sodium is reabsorb actively by sodium-potassium ATPase pumps. About 25 percent of the sodium, chloride and potassium are reabsorbed in the TAS. The LAS has a low reabsorptive capacity and does not reabsorb significant amounts of any of the substances.
The DCT also is virtually impermeable to water and urea, and avidly reabsorbs most of the ions. The transport of ions is done by the sodium-potassium ATPase pumps and the sodium-chloride co-transporter. Approximately 5 percent of the sodium and chloride is reabsorbed in this part.
The CNT is almost completely impermeable to water and urea. The CNT reabsorbs sodium ions and the rate of this reabsorption is controlled by hormones. The CNT also actively reabsorbs hydrogen ions by the hydrogen-ATPase mechanism and this plays a key role in the acid-base regulation of the body fluids.
The CD reabsorbs less than 10 percent of the filtered water, however, it plays an important role in determining

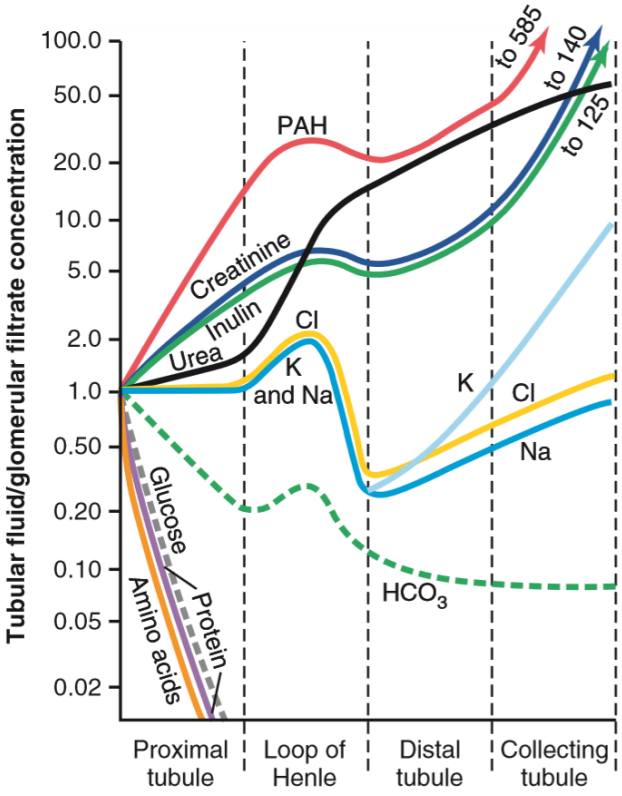

Figure 7: Normalized concentration of substances along the different parts of the nephron. A value of 1 corresponds to a concentration of the substance in the tubular fluid that is the same as the concentration of the substance in the plasma. Obtained from [10].

the final urine output. The water permeability of the CD is controlled by the antidiuretic hormone (ADH). If the level of ADH rises the water permeability of the CD increases and more water is reabsorbed into the interstitial fluid, thereby concentrating the urine. The CD also plays a role in the regulation of the acid-base balance, because it is capable of secreting hydrogen ions against large concentration gradients.
In Fig. 7 an overview of the concentrations of different substances along the different parts of the nephron is given. The concentration of a substance is normalized by the concentration of the substance in the blood plasma. When more water is reabsorbed than solute, the concentration of that solute increases and vice versa. In the figure we see, e.g., that glucose and amino acids are (approximately) completely reabsorbed in the proximal tubule. It is known that Inulin is not reabsorbed nor secreted along the tubular part, and therefore the concentration of this substance is an indicator of amount of water present in the tubular fluid.

3 Michaelis Menten kinetics

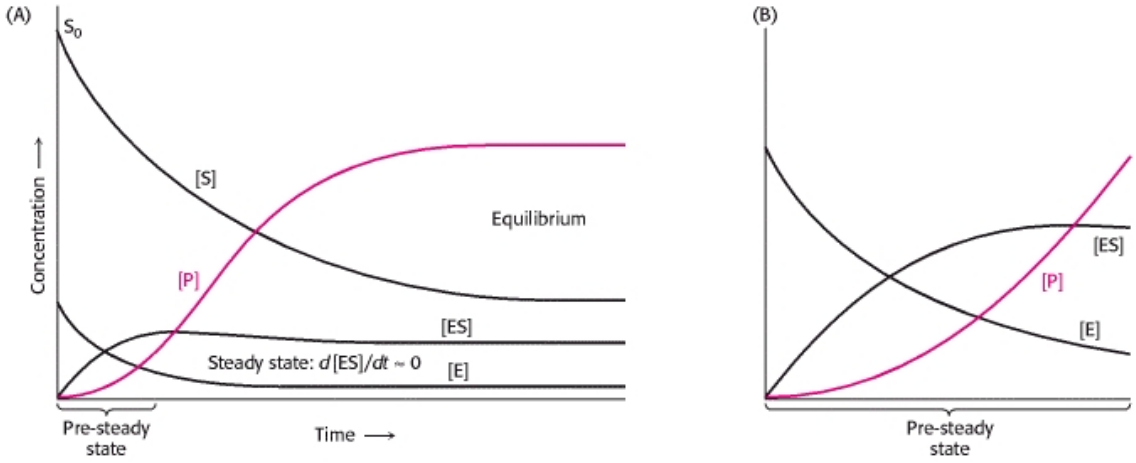

Figure 8: Concentration profiles of the different reaction participants of the reaction in Eq. (3) on a short (B) and a long (A) timescale. Taken from [27].

The sodium pumps in the kidney are commonly described by Michaelis-Menten kinetics, as mentioned in Sec. 2.1.4. In this section we will give a derivation of the Michaelis-Menten kinetics. In the original paper, L. Michaelis and M. L. Menten introduced this type of kinetics in a sligthly different notation than is used nowadays [28]. In the derivation we will use the notation used in [27] because we will largely follow the derivation given in Sec. 8.4 of this book. In the derivation we will make some assumptions and remarks that are applicable to the system we will study.
Consider a general system where an enzyme E forms an enzyme substrate complex ES with some kind of substrate S. From this ES the original E and a product P are formed. Written as a chemical reaction:

$$\mathrm{E} + \mathrm{S} \underset{\mathrm{k_{-1}}}{\overset{\mathrm{k_1}}{\rightleftharpoons}} \mathrm{ES} \underset{\mathrm{k_{-2}}}{\overset{\mathrm{k_2}}{\rightleftharpoons}} \mathrm{E} + \mathrm{P},$$

where the k_i's are the reaction rates for the different reactions. Now we will consider the case where the concentration of the substrate ($[S]$) is very high, so the concentration of the product ($[P]$) is low compared to $[S]$. In this case the reaction from the right hand side of Eq. (3) to ES is negligible.[7] We can therefore simplify the reaction equation to

$$\mathrm{E} + \mathrm{S} \underset{\mathrm{k_{-1}}}{\overset{\mathrm{k_1}}{\rightleftharpoons}} \mathrm{ES} \overset{\mathrm{k_2}}{\rightarrow} \mathrm{E} + \mathrm{P}\,. \tag{3.1}$$

We want to get an expression of the rate of formation (V) of the product P. Because this rate of formation is simply the reaction rate constant k times the concentration of the reactants, we can write

$$V = k_2[ES]. \tag{3.2}$$

Now we want to express $[ES]$ in terms of known quantities, i.e., in terms of $[S]$ and the total enzyme concentration $[E]_{tot} = [E] + [ES]$. We can write the rates of formation and breakdown of ES in the same way as Eq. (3.2) this gives:

$$\text{Formation rate } ES = k_1[E][S], \tag{3.3}$$
$$\text{Breakdown rate } ES = (k_{-1} + k_2)[ES]. \tag{3.4}$$

[7] In the system we study, $[S]$ remains at a high level because we have a flux going into the system with a high $[S]$. On the other hand there is a flux of P out of the system and this keeps $[P]$ fairly low. In fact the chemical reaction given by Eq. (3) will never reach its equilibrium concentrations because of these in and out fluxes.

Now we will make an additional assumption, viz., the steady-state assumption. This means that the concentration of the intermediate $[ES]$ is presumed to be constant regardless of the other concentrations. In Fig. 8 we see that after some time the steady state is reached, here $d[ES]/dt \approx 0$. If the reaction is in a steady state it means that the formation and breakdown rate are equal. Setting Eqs. (3.3) and (3.4) equal:

$$\begin{aligned} k_1[E][S] &= (k_{-1} + k_2)[ES] \quad \text{or} \\ \frac{[E][S]}{[ES]} &= \frac{(k_{-1} + k_2)}{k_1}. \end{aligned} \tag{3.5}$$

We define the constant K_m as[8]

$$K_m = \frac{(k_{-1} + k_2)}{k_1},$$

this constant is called the Michaelis constant. Plugging this constant into Eq. (3.5) and rewriting we arrive at an expression for [ES]:

$$[ES] = \frac{[E][S]}{K_m}. \tag{3.6}$$

We can write the total concentration of E ($[E]_{tot}$) as the sum of the concentrations of the free enzyme and the concentration of the enzyme in the complex ES, viz., $[E]_{tot} = [E] + [ES]$. We can write a similar expression for the total concentration of S ($[S]_{tot}$). The concentration $[S]$, however, is much lager than $[ES]$, i.e., $[S]_{tot} \approx [S]$. Therefore we can use that $[S]_{tot} = [S]$. Plugging this expression for $[E]_{tot}$ in Eq. (3.6) and solving for [ES] yields

$$\begin{aligned} [ES] &= \frac{([E]_{tot} - [ES])[S]}{K_m}, \\ &= \frac{[E]_{tot}[S]/K_m}{1 + [S]/K_m}, \\ &= [E]_{tot}\frac{[S]}{[S] + K_m}. \end{aligned} \tag{3.7}$$

Substituting expression (3.7) into Eq. (3.2) gives

$$V = k_2[E]_{tot}\frac{[S]}{[S] + [K]}. \tag{3.8}$$

When all the enzymes are in an enzyme substrate complex, i.e. when $[ES] = [E]_{tot}$, the maximum rate of formation (V_m) of P is attained. If we look at Eq. (3.2) we can easily see that $V_m = k_2[E]_{tot}$. Plugging this definition of V_m in Eq. (3.7) we we get the well-known Michaelis-Menten equation:

$$V = V_m\frac{[S]}{[S] + K_m}. \tag{3.9}$$

In Fig. 9 a plot is shown of the $[S]$-dependence of rate V that obeys equation (3.9). In the plot we see that for a concentration $[S] = K_m$ the reaction rate $V = V_m/2$, which can also obviously be seen form Eq. (3.9). The sodium pumps in the kidney are commonly described by Michaelis-Menten kinetics [25, 26]. We will therefore also use these kinetics to describe the sodium pumps in our model. In our model, the concentration of sodium ions in the tube is equivalent to the substrate concentration $[S]$, the ion pumps play the role of the enzymes E_{tot}, and the concentration of ions in the interstitium is equivalent to the concentration of the product $[P]$. Although the ions in both the tube and interstitium are sodium ions (no chemical reactions take place) we can describe them in terms of a substrate and a product concentration. This is because the sodium pumps can only pump ions from the tube to the interstitium and therefore are only dependent on $[S]$. We will use Eq. (3.9) to define a flux from the tubule to the interstitium. Note that V (and V_m) has units mol/(m^{3}s), but we can also express V_m in mol/(m^{2}s) to get a flux.[9]

[8] K_m is an important characteristic of these type of equations and is independent of $[E]$ and $[S]$. K_m has unit of concentration.
[9] This is what Sophie Marbach used in her model [17] and what we will use in our model.

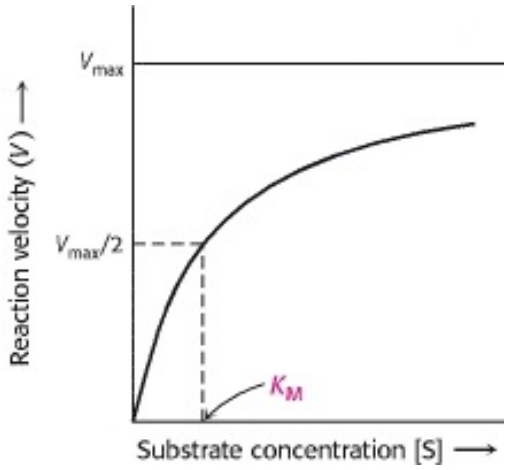

Figure 9: Rate of formation (V) as a function of the substrate concentration [S] for an enzyme that obeys Michaelis-Menten kinetics. Taken from [27]

Now, a pump may also pump multiple molecules at the same time. As shown by Garay and Garrahan the above equation can be generalized to the case where n sites can be occupied/pumped on each pump unit [25]:

$$V = nV_m \left(\frac{[ion]_A}{K_m + [ion]_A} \right)^n , \tag{3.10}$$

where V_m is the same as in Eq. (3.9) and the extra n comes from the fact that n molecules are pumped at the same time.
Values for relevant parameters are chosen as follows: $L = 1$ mm, $R = 10$ m, $\eta = 0.69$ mPa·s and $\Delta p = 33$ Pa

4 Poisson-Nernst-Planck-Stokes equations

In this section we will give and discuss the equations that we need to describe a system of electrolytes flowing through (small) canals with possibly charged surfaces. Here, we largely follow the discussion of section 9.3 of Ref. [29].

4.1 Continuity equation

We will only consider systems where no chemical reactions take place and hence the number of particles of each species is conserved. Because every particle has a fixed mass, this quantity will also be conserved. The conservation of mass (of each species) is describe by the continuity equation, in which the density $\rho_i(\boldsymbol{r}, t)$ and flux $\boldsymbol{J_i}(\boldsymbol{r}, t)$ of particles at position $\boldsymbol{r}$ and time t are related as follows

$$\frac{\partial \rho_i(\boldsymbol{r}, t)}{\partial t} + \nabla \cdot \boldsymbol{J_i}(\boldsymbol{r}, t) = 0, \tag{4.1}$$

where label i indicates the different species. For a detailed derivation of the continuity equation see appendix A.

4.2 Flux equation

The next equation we need to describe the system, is a relation between the flux and the different forces that acts on our system. We consider four different contributions to the flux: (i) the diffusive flux $\boldsymbol{J}_i^{dif} = -D_i \nabla \rho_i$ due to local density gradients, (ii) the conductive flux $\boldsymbol{J}_i^{cond} = \rho_i \boldsymbol{v}_i$ that stems from the electric force experienced by a paticle in an electric field $\boldsymbol{E}(\boldsymbol{r}, t)$ and (Stokesian) friction, this can be rewritten as $\boldsymbol{J}_i^{cond} = (D_i/k_B T) z_i e \rho_i \boldsymbol{E}$ (ii) the conductive flux $\boldsymbol{J}_i^{cond'} = -(D_i/k_B T)\rho_i \nabla U_i$ due to a non-electric external potential $U_i(\boldsymbol{r})$, (iv) the convective flux $\boldsymbol{J}_i^{conv} = \rho_i \boldsymbol{u}$ simply from the fact that a fluid may flow with velocity $\boldsymbol{u}$. Below we will comment on each contribution.
(i) For a detailed derivation see B. Note that this relation is different for every particle species and therefore the index i is introduced.
(ii) + (iii) In general we can describe the acceleration $\boldsymbol{v}_i$ of a particle by Newton's law $\boldsymbol{F}_i = m\dot{\boldsymbol{v}}_i$. However, the inertia term can be omitted if we consider a system with a small length scale L, i.e. Re $= muL/\eta < 1$, where m is the mass density of the fluid, L the length scale of the system and η the viscosity of the fluid.[10] If we omit this inertia term we are left with $\boldsymbol{F}_i = 0$. This means that a particle will only move if we exert a force on it. The forces that may act on a (charged) paticle are:
The electric force is given by $\boldsymbol{F}_i^{el} = z_i e \boldsymbol{E}$, where the valency z_i takes positive values for positively charged particles and negative values for negatively charged particles. This guarantees that the sign of $\boldsymbol{F}_i^{el}$ is correct.
The next force is a force that may be present in our system due to any external potential, in general this force is given by $\boldsymbol{F}_i^{ext} = -\nabla U_i$, where U_i can be any non-electric external potential that acts on particle species i.
A particle experiences a friction force if it has a speed relative to the flow of the solvent. We will use the Stokes friction for the particles in our system $\boldsymbol{F}_i^{Stokes} = -6\pi\eta a_i \boldsymbol{v}_i$, where η is the solvent viscosity a_i is the (hydrodynamic) radius of ionic species i. For a derivation of this Stokes friction see section 7.2 of [30]. Note that in this section the assumption is that the particles are spherical, which is also applicable to our system because we will mostly only consider particles like Na^+, K^+ and Cl^-, which can be approximated to be spherical.
Putting together all force contributions and using $\boldsymbol{F} = 0$ we get

$$6\pi\eta a_i \boldsymbol{v}_i = z_i e \boldsymbol{E} - \nabla U_i. \tag{4.2}$$

Rewriting this to get an expression for the force in terms of all other quantities in our system results in

$$\boldsymbol{v}_i = \frac{z_i e \boldsymbol{E}}{6\pi\eta a_i} - \frac{\nabla U_i}{6\pi\eta a_i}. \tag{4.3}$$

[10] A typical value for Re in the model we will build is Re $\approx 10^3 * 10^-4 * 10^-3/10^-3 = 0.1$. See Note 13 in Sec. 4.4 for more information of the Reynolds number.

Define $\boldsymbol{v}_i = \boldsymbol{v}_i^{cond} + \boldsymbol{v}_i^{cond'}$, where $\boldsymbol{v}_i^{cond}$ denotes the contribution to the relative speed of particle species i due to the electrical force and $\boldsymbol{v}_i^{cond'}$ the contribution due to non-electrical forces. In general the flux is defined as $\boldsymbol{J}_i = \rho_i \boldsymbol{v}_i$ and therefore we can write the conductive fluxes in terms of the velocities defined above. This result in $\boldsymbol{J}_i^{cond} = \rho_i \frac{z_i e \boldsymbol{E}}{6\pi\eta a_i}$ and $\boldsymbol{J}_i^{cond'} = -\rho_i \frac{\nabla U_i}{6\pi\eta a_i}$. Using the Stokes-Einstein relation $D_i = \frac{k_B T}{6\pi\eta a_i}$, [11] the equations for the fluxes can be rewritten in terms of the diffusion constant D_i as

$$\boldsymbol{J}_i^{cond} = \frac{D_i}{k_B T}\rho_i z_i e \boldsymbol{E} \qquad \text{and} \qquad \boldsymbol{J}_i^{cond'} = -\frac{D_i}{k_B T}\rho_i \nabla U_i \tag{4.4}$$

(iv) The fluid flow is a flow of all the particles, i.e. solvent plus solutes, together with a velocity $\boldsymbol{u}$ and from this there is an advective contribution to the flux of every particle that is simply given by the density times this velocity $\boldsymbol{u}$.

Putting together all terms that contributes to the flux gives us the next equation:

$$\boldsymbol{J_i} = -D_i(\nabla\rho_i + z_i\rho_i\beta e\nabla\psi + \rho_i\beta\nabla U_i) + \rho_i\boldsymbol{u}. \tag{4.5}$$

4.3 Poisson equation

Because in our system we are dealing with charged particles (ions) we need an additional equation that describes the electrostatics of those particles. We also see that Eq. (4.5) is in terms of the unknown electrostatic potential ψ. The additional relation we need, that describes the electrostatics of our system, is the Poisson equation

$$\epsilon_0\epsilon\nabla^2\psi = -Q_{ext} - e\sum_i z_i\rho_i, \tag{4.6}$$

where ϵ_0 and ϵ are the absolute permittivity of vacuum and of the dielectric medium of our system, respectively, and $Q_{ext}(\boldsymbol{r}, t)$ is the (non-ionic) external charge. The external charge can be incorporated as in the equation above.
This equation describes a system where the dielectric medium is homogeneous, i.e. ϵ is a constant. A detailed derivation of this equation can be found in Ref. [31]

4.4 Stokes equation

In Eq. (4.5) we still have an unknown flow velocity $\boldsymbol{u}$. This velocity can be calculated by solving the Navier-Stokes equation. For an incompressible isotropic fluid this equation is

$$m\frac{\partial \boldsymbol{u}}{\partial t} + m(\boldsymbol{u}\cdot\nabla)\boldsymbol{u} = -\nabla p + \eta\nabla^2\boldsymbol{u} + \boldsymbol{f}; \qquad \nabla\cdot\boldsymbol{u} = 0, \tag{4.7}$$

where m is the (constant) mass density, $p(\boldsymbol{r}, t)$ the local pressure, and $\boldsymbol{f}(\boldsymbol{r}, t)$ an additional body force. A detailed derivation of the Navier-Stokes equation can be found in Ch. 6 of [30]. We will almost always only consider electrostatic forces. In this case the force is given by Coulomb's law and thus $\boldsymbol{f}(\boldsymbol{r}, t) = -e\sum_i z_i\rho_i(\boldsymbol{r}, t)\nabla\psi(\boldsymbol{r}, t)$. [12] The relation $\nabla\cdot\boldsymbol{u} = 0$ is known as the incompressibility condition and is actually a conservation law. Below we will derive this incompressibility condition.
The requirement for a fluid to be incompressible means that ρ is constant within a small volume element which moves at the flow velocity $\boldsymbol{u}$. We start from the continuity equation 4.1 and use that the flux is related to the flow velocity by $\boldsymbol{J} = \rho\boldsymbol{u}$. This gives us the following equation:

$$\frac{\partial\rho}{\partial t} + \nabla\cdot(\rho\boldsymbol{u}) = \frac{\partial\rho}{\partial t} + \nabla\rho\cdot\boldsymbol{u} + \rho(\nabla\boldsymbol{u}) = 0. \tag{4.8}$$

[11] For a detailed derivation of this equation see section 4.1-4.3 of [29]

[12] Start from Coulomb's law $\boldsymbol{F} = k_e\frac{Qq}{|r|^2}\hat{r}$, where $\boldsymbol{F}$ is the force between a charge Q and another charge q at a distance r. Make a superposition for all (charged) particles, i.e. $\boldsymbol{F} = \boldsymbol{F_1} + \boldsymbol{F_2} + \ldots = Q\left(\frac{k_e q_1}{|r_1|^2}\hat{r}_1 + \frac{k_e q_2}{|r_2|^2}\hat{r}_2 + \ldots\right)$. Now the electric field is $\boldsymbol{E} = \sum_i \frac{k_e q_i}{|r_i|^2}\hat{r}_i$, and define the potential $\boldsymbol{E} = -\nabla\psi$. This together results in $\boldsymbol{F} = -Q\nabla\psi$, to get the desired result set $Q = ez_i\rho_i$ and sum over all particle species.

Now, instead of the rate of change of ρ on a fixed position, we calculate the rate of change of ρ 'following the fluid'. This can be calculated using the total derivative, or material derivative which we denote $\frac{Df}{Dt}$ and this is define as

$$\frac{D\rho}{Dt} = \frac{\partial \rho}{\partial t} + \frac{\partial \rho}{\partial x}\frac{dx}{dt} + \frac{\partial \rho}{\partial y}\frac{dy}{dt} + \frac{\partial \rho}{\partial z}\frac{dz}{dt}.$$

Now the change of $x(t)$, $y(t)$ and $z(t)$ 'following the fluid' is equal to the local flow velocity $\boldsymbol{u} = (u, v, w)$:

$$\frac{dx}{dt} = u, \qquad \frac{dy}{dt} = v, \qquad \frac{dz}{dt} = w.$$

So if we follow a volume element that is moving with the fluid flow, the total derivative is

$$\frac{D\rho}{Dt} = \frac{\partial \rho}{\partial t} + \nabla\rho \cdot \boldsymbol{u}.$$

Using Eq. (4.8) we can rewrite this expression to

$$\frac{D\rho}{Dt} = -\rho(\nabla \cdot \boldsymbol{u})`.$$

Now because we only consider incompressible fluids the change in density over time needs to be zero (if it is not zero the fluid is compressed or expanded). This means that the material derivative of the density vanishes and therefore also the divergence of the flow velocity. This results in the incompressibility condition of Eq. (4.7)
Eq. (4.7) can be simplified in most of our cases of interest. Because in the systems we will study, the viscous forces will be strong and therefore the velocities are small. To determine which terms in Eq. (4.7) are relevant, if we are in a system with strong viscous forces, we use the Reynolds number $\mathrm{Re} = muL/\eta$. [13] In the case that $\mathrm{Re} \ll 1$ the inertia-term can be omitted and this results in the incompressible Stokes equation

$$\begin{aligned} m\frac{\partial \boldsymbol{u}}{\partial t} &= -\nabla p + \eta\nabla^2\boldsymbol{u} - e\sum\nolimits_i z_i\rho_i\nabla\psi \\ &= -\nabla p + \eta\nabla^2\boldsymbol{u} + \epsilon_0\epsilon(\nabla^2\psi)\nabla\psi; \qquad \nabla\cdot\boldsymbol{u} = 0, \end{aligned} \tag{4.9}$$

where we rewrote the first line using the Poisson equation (Eq. (4.6)).
The equations (4.1), (4.5), (4.6), (4.9) form the Poisson-Nernst-Planck-Stokes equations.

4.5 Example: Poiseuille flow

We will give one example of the above theory, because we will use this quiet often in our model. Consider a cylindrical tube of length L and radius R ($L \gg R$) and an applied pressure drop Δp between the top and bottom of the cylinder, see Fig. 10. For convenience we will use cylindrical coordinates. The fluid in the tube is solute-free and is pushed through the tube by this applied pressure. We are interested in the stationary situation and there are no other forces acting on the system, so the resulting Stokes equation[14] is:

$$\eta\nabla^2\boldsymbol{u}(\boldsymbol{r}) - \nabla p(\boldsymbol{r}) = \boldsymbol{0}, \qquad \nabla\cdot\boldsymbol{u}(\boldsymbol{r}) = 0. \tag{4.10}$$

The geometry is rotational symmetric, so we expect no flow in the φ-direction and also no dependence on the φ-direction. Because $L \gg R$ we can ignore inlet and outlet effects and then it follows by symmetry that $\boldsymbol{u}(\boldsymbol{r}) = (0, 0, u_z(r, z))$. From the incompressibility condition $\nabla\cdot\boldsymbol{u} = \partial u_z/\partial z = 0$ it follows that there is no z-dependence. So the Stokes equation 4.10 of our problem reduces to:

$$\eta\frac{1}{r}\frac{\partial}{\partial r}\left(r\frac{\partial u_z(r)}{\partial r}\right) - \frac{\partial p(z)}{\partial z} = 0, \tag{4.11}$$

[13] The inertia term $(m\boldsymbol{u}\cdot\nabla)\boldsymbol{u}$ is of order $O(mu^2/L)$ and the viscous term $\eta\nabla^2\boldsymbol{u}$ of order $O(\eta u/L^2)$ and the ratio of those terms *inertia/viscous* is of order $O((mu^2/L)/(\eta u/L^2)) = O(\mathrm{Re})$. [30]
[14] we are implicitly assuming that the Reynolds number $Re \ll 1$

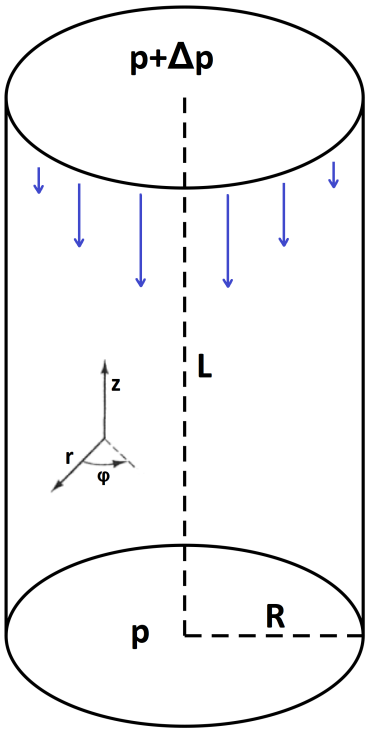

Figure 10: Cylindrical tube filled with fluid. On the top of the cylinder is a higher pressure, resulting in a pressure gradient of Δp between top and bottom. The blue arrows indicates the resulting Poiseuille flow.

where we have written the Laplacian in cylindrical coordinates. If we take the derivative of this equation w.r.t. z we get $\partial^2 p(z)/\partial z^2 = 0$, which means that $\partial p(z)/\partial z = constant = \Delta p/L$. To solve Eq. (4.11) we need boundary conditions. The boundary conditions of our system are given by a no-slip condition on the wall and a condition of axial symmetry on $r = 0$.

$$u_z(r = R) = 0, \qquad \left.\frac{\partial u_z(r)}{\partial r}\right|_{r=0} = 0. \tag{4.12}$$

We solve Eq. (4.11) in the following steps:

$$\begin{aligned}
\frac{\eta}{r}\frac{\partial}{\partial r}\left(r\frac{\partial u_z(r)}{\partial r}\right) &= \frac{\partial p(z)}{\partial z}, \\
\frac{\partial}{\partial r}\left(r\frac{\partial u_z(r)}{\partial r}\right) &= \frac{r}{\eta}\frac{\partial p(z)}{\partial z}, \\
&\textit{Integrate both sides w.r.t. } r, \\
r\frac{\partial u_z(r)}{\partial r} &= \frac{r^2}{2\eta}\frac{\partial p(z)}{\partial z} + C_1, \\
\frac{\partial u_z(r)}{\partial r} &= \frac{r}{2\eta}\frac{\partial p(z)}{\partial z} + \frac{C_1}{r}, \\
&\textit{Integrate both sides w.r.t. } r, \\
u_z(r) &= \frac{r^2}{4\eta}\frac{\partial p(z)}{\partial z} + C_1 \ln r + C_2.
\end{aligned} \tag{4.13}$$

Now apply the condition of axial symmetry to the above equation and get:

$$\left.\frac{\partial u_z(r)}{\partial r}\right|_{r=0} = \left[\frac{r}{2\eta}\frac{\partial p(z)}{\partial z} + C_1\frac{1}{r}\right]_{r=0} = 0.$$

From this it follows that $C_1 = 0$. And last but not least we apply the no-slip boundary condition to the resulting equation above.

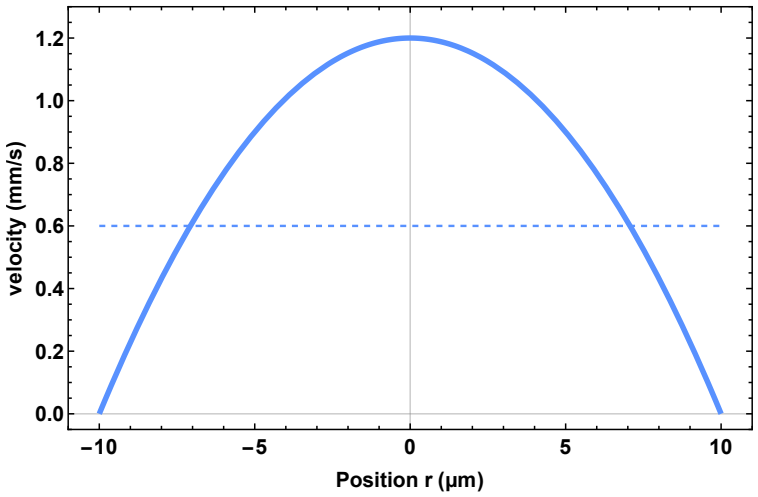

Figure 11: Poiseuille flow velocity profile (solid blue line) and corresponding average velocity (dashed blue line). Values for relevant parameters are chosen as follows: $L = 1$ mm, $R = 10$ μm, $\eta = 0.69$ mPa·s and $\Delta p = 33$ Pa. All parameters are in the order of magnitude of the model that we are going to build.

$$u_z(r)\Big|_{r=R} = \left[\frac{r^2}{4\eta}\frac{\partial p(z)}{\partial z} + C_2\right]_{r=R} = \frac{R^2}{4\eta}\frac{\partial p(z)}{\partial z} + C_2,$$

from this we conclude that $C_2 = -\frac{R^2}{4\eta}\frac{\partial p(z)}{\partial z}$. Plugging this C_2 in Eq. (4.13) yields the so-called Poiseuille flow profile:

$$u_z(r) = -\frac{(R^2 - r^2)}{4\eta}\frac{\partial p(z)}{\partial z}. \tag{4.14}$$

The average velocity can be obtained by integrating Eq. (4.14) over the surface of cross-section of the tube and divide this by the surface area.

$$\begin{aligned} u_{avg} &= \frac{1}{\pi R^2}\int_0^R\int_0^{2\pi} u_z(r) r\, d\phi dr, \qquad (4.15)\\ &= \frac{2\pi}{\pi R^2}\int_0^R \left(-\frac{(R^2 - r^2)}{4\eta}\frac{\partial p(z)}{\partial z}(r) r\right) dr,\\ &= -\frac{2}{R^2}\left[\left(\frac{R^2 r^2}{8\eta} - \frac{r^4}{16\eta}\right)\frac{\partial p(z)}{\partial z}\right]_{r=0}^{r=R},\\ &= -\frac{2}{R^2}\left(\frac{R^4}{16\eta}\frac{\partial p(z)}{\partial z}\right),\\ &= -\frac{R^2}{8\eta}\frac{\partial p(z)}{\partial z}. \qquad (4.16) \end{aligned}$$

In the description of the model we will use the Poiseuille flow profile and average Poiseuille flow velocity.

5 Building blocks for kidney model

In this section we describe the building blocks we made for a 3D model of the kidney. In Sec. 2 we gave a detailed description of the kidney. In the model we use a simplified geometry compared to the real (human) kidney that we will explain first. We are using a geometry consisting of 3 parallel tubes with the same length and diameter, which are connected as in Fig. 12. Note that this geometry is also shown in the introduction (Sec. 1). Between the tubes there is something called the interstitium (I), in this part the fluid and solutes can flow freely. In our model I is open at the top and closed at the bottom, so the fluid and solutes can only flow out of I at the top. The first tube is called the descending tube (D) and the cells lining this tube are permeable to water and impermeable to solutes. The second tube is the ascending tube (A) and the cells of this tube can actively pump water from the tube, but the cells are impermeable to water. The last tube is called collecting duct (CD), this tube has the same properties as D.

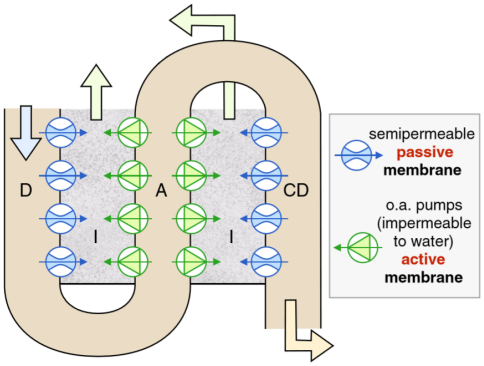

Figure 12: Geometry used in [17], consisting of 3 different tubules: descending tube (D), ascending tube (A) and collecting duct (CD). The interstitium (I) surrounds all tubules. Arrows indicate the direction of the flux of the fluid. Note that the properties of D and CD are exactly the same in the model.

We assume that the tubes are rotational symmetric (symmetric in the φ-direction), so we can do the numerical calculations in a 2D-axisymmetric geometry instead of a fully 3D geometry. The advantages of this are that the numeric calculations are a lot faster and that the solutions are indeed axisymmetric. If we would use a fully 3D model, the numerical calculations could, due to numerical errors, also result in small effects in the φ-direction that should not be present. We study the steady state of the system, i.e. $(\partial x)/(\partial t) = 0$ for every quantity x, and do not include any chemical reaction.

Below we will discuss how we modelled tube D (and CD[15]) and tube A in COMSOL and show the results of numerical calculations. In both sections we will start with some physical considerations. Then we give a description of the geometry and some COMSOL-specific aspects. After that we discuss the set of equations and boundary conditions we solved. And at the end we show the results of the numerical calculations.

We also tried to connect the different tubes to get a complete model of the kidney. But we did not have much time for this step and we have encountered several problems by doing this. Therefore we do not discuss this here, but we will give a short explanation in the discussion (Sec. 6.2).

5.1 Descending tube

The descending tube (same for CD) is permeable to water and impermeable to all the solutes. So in this tube the solution gets increasingly concentrated. The geometry we use to model D can be found in Fig. 13.

5.1.1 Physical considerations

Marbach and Bocquet use the hydraulic conductivity P_f (unit: m/s) in their model to described the permeable wall. We use a porous media domain in COMSOL which is characterized by a porosity ϵ_p and a permeability κ. The porosity is the fraction of the volume of voids (or empty spaces) over the total volume. The relation between P_f and κ is given by:

$$\kappa = P_f \frac{\mu}{\rho g}, \tag{5.1}$$

where μ is the (dynamic) viscosity, ρ the density and g the acceleration due to gravity. The value for the hydraulic conductiviy used by Marbach and Bocquet is $P_f = 2500$ µm/s [6]. If use this value for P_f and the following values for the other parameters: $\mu = 1$ mPa·s, $\rho = 998$ kg/m^3 and $g = 9.81$ m/s^2 we get

[15] In our discussion in Sec. 5.1 we will only talk about tube D. But for tube CD the same model applies.

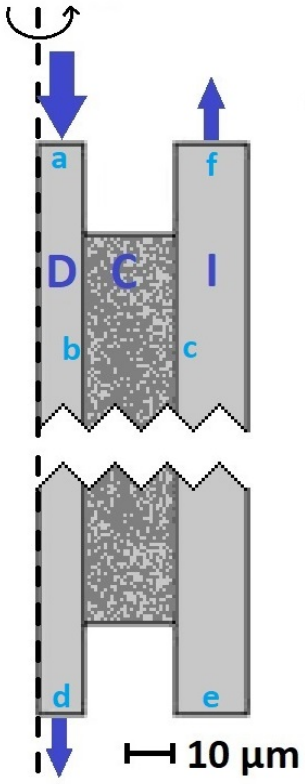

Figure 13: Geometry used in the numerical calculations for the water permeable wall. The blue arrows indicate in- and outflux of water. D stands for descending tube, C for the cells lining this tube and I for the interstitium around this tube. Domain C is permeable to water, but not to ions. Note that this is a shortened version (real length is in the order of 1 mm) of the real geometry as indicated by the jagged line.

$\kappa = 2.6 \cdot 10^{-12}$ m^2. All parameters values used above are values that are also used in our model.
We also include ions in the descending tube and expect to get the same flux of ions going in and out the tube because the semi-permeable wall of this tube is impermeable to ions. The ions are necessary to include, because the fluid flow from the descending tube to the interstitium is driven by osmosis. The process of osmosis depends on the concentration difference between the tube and the interstitium.

5.1.2 COMSOL

To model the fluid flow and the permeable wall in D we use the *Creeping Flow* module in COMSOL. For domain C we define a domain of porous media (*Fluid and Matrix Properties* in COMSOL) and use this, to certain extend, as a black box. We control the parameters ϵ_p and κ that characterizes this domain, but we are not to much concerned with the exact equations that are being solved. Therefore we do not give any set of equations for domain C in the section below. In the discussion (Sec. 6.2) we will comment on this choice. To also include ions in the descending tube we use the *Transport of Diluted Species* module. We first solve the *Creeping Flow* module and use the results as input for the calculations in the *Transport of Diluted Species* module.

5.1.3 Equations and boundary conditions

We will now give, and where necessary explain, the equations and boundary conditions we will solve. We solve the *Creeping Flow* module, which means that we solve the following equations for domain A and I:

$$\begin{aligned} -\nabla p + \eta \nabla^2 \boldsymbol{u} &= 0, \\ \nabla \cdot \boldsymbol{u} &= 0. \end{aligned} \tag{5.2}$$

The boundary conditions are:

$$\begin{aligned} \text{a)} &\quad \text{Inlet pressure } p_{in}, \\ \text{d, f)} &\quad \text{Either a pressure condition } p_{out}, \text{ or an open boundary (no normal stress) } f_n = 0, \\ \text{other boundaries)} &\quad \text{All other boundaries are hard walls (no normal flux) with a no-slip boundary condition.} \end{aligned} \tag{5.3}$$

Note that wall b and c are no boundaries in this model, because domain C is connected to A and I. As mentioned above we will not write down the equations for domain C. This domain is characterized by ϵ_p and κ, where $\sqrt{\kappa}$ is a characteristic length scale for the system.
After we solve the *Creeping Flow* module, we solve the *Transport of Diluted Species* module and use the calculated velocity profile as an input for this module. We solve the following set of equations:

$$\begin{aligned} \boldsymbol{J^{ion}} &= -D^{ion}\nabla\rho^{ion} + \boldsymbol{u}\rho^{ion}, \\ \nabla \cdot \boldsymbol{J^{ion}} &= 0. \end{aligned} \tag{5.4}$$

Note that we only solve these equations in domain D, because the boundary between D and C is impermeable to water and we only want to calculate the concentration profiles of the ions in D. The boundary conditions of this system are:

$$\begin{aligned} \text{a)} &\quad \text{initial concentration } \rho_0^{ion}, \\ \text{d)} &\quad \text{no diffusive flux } \boldsymbol{n} \cdot D^{ion}\nabla\rho^{ion}, \\ \text{other boundaries)} &\quad \text{All other boundaries are hard walls with a no-flux boundary condition.} \end{aligned} \tag{5.5}$$

The no-flux boundary condition (on d) can be applied because $\boldsymbol{J_{adv}^{ion}} \gg \boldsymbol{J_{dif}^{ion}}$ as shown in Sec. 5.2.1. The normal vector to any boundary is $\boldsymbol{n}$ and D^{ion} is the diffusion coefficient of ions in water.

5.1.4 Results

The way we built the model for the descending tube turned out to be not the right way and therefore we will only shortly show some results. The reason why this way of modeling the descending tube is not the right way, is that the flux of ions is not conserved along the tube. This problem will be discussed more extensive in the discussion (Sec. 6.2). Also, the flux going out of the interstitium (light orange line in Fig. 14) is to high; this will be discussed below.
In Fig. 14 we see the resulting normalized fluxes of the model for an applied pressure $p_{in} = 1000$ Pa on the inlet of the descending tube (D) and open boundaries at the outlet of the tube and the interstitium. In our model $R_T = 10$ µm is the radius of the tube, $R_C = 20$ µm the diameter of the cells (domain C in Fig. 13) and $R_I = 12$ µm the diameter of I. The values for m, η and D^{ion} can be found in Tab. 3 in Sec. 5.2.4. In Fig. 14 we see that the normalized flux going out of I is significantly higher for the 3D geometry than for the 2D geometry. in Fig. 14 we see that for $\kappa = 2.6 \cdot 10^{-12}$ m^2 the normalized flux going out of I (light orange) is almost 1. However, in the calculations of Marbach and Bocquet this values is ~ 0.9, this means that the flux that follows from out calculations is to high. This is due to the fact that the pressure difference between the inlet of D and outlet of I is to high, we therefore applied a lower pressure p_{in} but the results from this calculations were not significantly different from the results in Fig. 14. We think the problem is due to the fact that we only applied a hydrostatic pressure and no osmotic pressure. The reason why we did not use a (proper) osmotic pressure in our model will be discussed in Sec. 6.2.

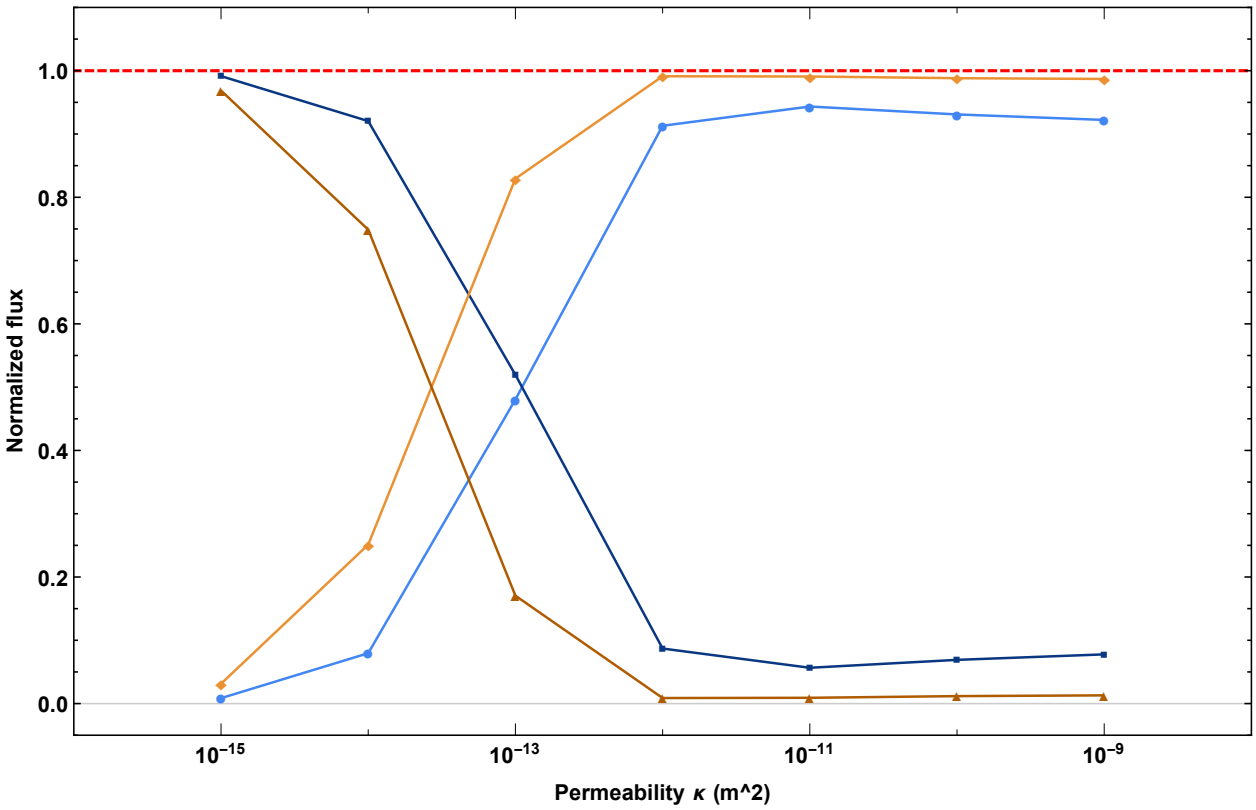

Figure 14: Normalized fluxes going out of the descending tube (D) of length $L = 0.5$ mm and radius $R_T = 10$ µm and out of the interstitium (I) of length L and radius $R_I = 50$ µm for a 2D and 3D geometry. Fluid flow is forced by an applied pressure of $p_{in} = 1000$ Pa on the inlet of D. The fluxes are normalized on the flux going into the descending tube. For the 2D geometry the normalized flux going out of I (light blue) is lower than this flux for the 3D geometry (light orange). The normalized flux going out of D for the 2D geometry (dark blue) is higher than this flux for the 3D geometry (dark orange).

5.2 Ascending tube

The ascending tube is the middle tube of Fig. 12 and this one contains the ion pumps. The ions are pumped actively from A to I, the water can not flow from A to I, so the solution is increasingly diluted along A. The geometry we use to model A can be found in Fig. 15.

5.2.1 Physical considerations

We want to build a model that only takes the sodium and chloride into account. We do not take into account the other ions that are also present in the kidney, because the concentrations of sodium and chloride are at least one order of magnitude larger than that of the other ions [11, 12]. In addition, we want to make a model that resembles the kidney, but not necessarily a model that is as realistic (and complicated) as possible. The sodium ions are pumped actively from the ascending tube to the interstitium, the kinetics for these pumps are described in Sec. 3. The chloride ions follows through the cell walls and diffuses to keep the system electroneutral [17, 32]. We will therefore only consider one type of ions in the system (the sodium ions) that do not have any charge.

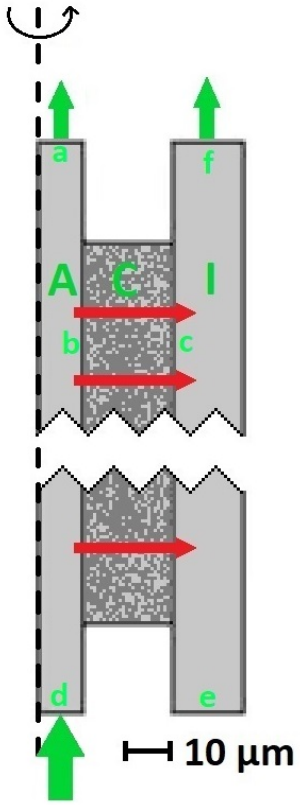

Figure 15: Geometry used in the numerical calculations for the ion-pumps. The green arrows indicate in- and outflux of ions. A stands for ascending tube, C for the cells lining this tube and I for the interstitium around this tube. The red arrows indicate the direction of the active ion pumping. The lowercase letters are used for the boundary conditions in Sec. 5.2.3. Note that this is a shortened version (real length is in the order of 1 mm) of the real geometry as indicated by the jagged line.

One may ask: how are the ions transported through the system? We already know that in domain C there are pumps, actively pumping the ions from A to I. In the other domains (A & I) the ions are transported by diffusion and convection. We calculate the contribution to the flux of both the diffusive and convective term. First we consider the flux in the direction parallel to the symmetry axis (the z-direction). The advective flux is given by $\boldsymbol{J}^{\boldsymbol{ion}}_{\boldsymbol{adv}} = \rho_{ion}\boldsymbol{u}$ and the diffusive flux by $\boldsymbol{J}^{\boldsymbol{ion}}_{\boldsymbol{dif}} = -D_{ion}\nabla\rho_{ion}$, see also Sec. 4.2. We will now estimate the order of magnitude of both flux terms. The density of the ions ρ_{ion} in our system is $\sim 10^2$ mol/m^3 and the flow velocity $\boldsymbol{u} \sim 10^{-4}$ m/s, so $\boldsymbol{J}^{\boldsymbol{ion}}_{\boldsymbol{adv}} \sim 10^{-2}$ mol/(m^{2}s). The diffusion coefficient D_{ion} of the ions in water is $\sim 10^{-9}$ m^2/s and the concentration gradient[16] $\nabla\rho_{ion} \sim 10^5$ mol/m^4, so $\boldsymbol{J}^{\boldsymbol{ion}}_{\boldsymbol{dif}} \sim 10^{-4}$

[16]The concentration gradient can be estimated by $\frac{\Delta\rho_{ion}}{L} \sim \frac{10^2}{10^{-3}} = 10^{-5}$ mol/m^4.

mol/(m^{2}s). We see that $\boldsymbol{J^{ion}_{adv}} \gg \boldsymbol{J^{ion}_{dif}}$ and therefore the driving force of the solute transport through the tubes is the fluid flow.
We also want a fluid flow in I to transport all the ions, that are actively pumped, out of the system. That means that we have to solve Eqs. 5.6 in domains A and I. If we do not, then the concentration of ions ρ^{ion} would go to infinity because the ion pumps are only dependent of ρ^{ion} in tube A.
In the direction perpendicular to the symmetry axis (r-direction) there is no pressure gradient and therefore diffusion in this direction is important. The timescale of this diffusion is $t_{dif} \approx R^2/(6D) = 10^{-10}/(6\cdot 10^{-9}) \approx 10^{-2}$ sec, the timescale of the advection of the particles through the tube is $t_{adv} = L/u_{avg} \approx 10^{-3}/10^{-4} = 10$ sec. We see that $t_{dif} \ll t_{conv}$, this means that the concentration of ions in the r-direction is approximately constant. In the results we also see this, as will be discussed below.

5.2.2 COMSOL

To model the ion-pumps[17] we used the geometry shown in Fig. 15. We use the modules *Creeping Flow* and *Transport of Diluted Species* to model the ascending tube. We need the module *Creeping Flow* to model the fluid flow that transports the solutes through the different tubes of the nephron. This is because the convective term of the flux ($\boldsymbol{J^{ion}_{conv}}$) is much larger than the diffusive term ($\boldsymbol{J^{ion}_{dif}}$) as shown in Sec. 5.2.1.[18]
We perform the calculations in two steps: first we search for a stationary solution for the fluid, i.e. doing a stationary study in COMSOL that solves for the equations and boundary conditions of the *Creeping Flow* module. The result of this calculation is then given as input for the next step. In this next step we let COMSOL search for a stationary solution of the *Transport of Diluted Species* module.

5.2.3 Equations and boundary conditions

We will now give, and where necessary explain, the equations and boundary conditions we will solve. First we solve the *Creeping Flow* module, which means that we solve the following equations:

$$\begin{aligned} -\nabla p + \eta \nabla^2 \boldsymbol{u} &= 0, \\ \nabla \cdot \boldsymbol{u} &= 0. \end{aligned} \tag{5.6}$$

Note that we only solve these equations in domain A and I, because C is impermeable to water. The boundary conditions of the system are:

$$\begin{aligned} \text{pair a+d)} \quad & \text{Either two pressures } p_0 + \Delta p_T \text{ and } p_0 \text{ or a velocity and an open boundary}[19] \\ & \text{(no normal stress) } u_T \text{ and } f_n = 0, \\ \text{pair e+f)} \quad & \text{Either two pressures } p_0 + \Delta p_I \text{ and } p_0 \text{ or a velocity and an open boundary} \\ & \text{(no normal stress) } u_I \text{ and } f_n = 0, \\ \text{other boundaries)} \quad & \text{All other boundaries are hard walls with a no-slip boundary condition.} \end{aligned} \tag{5.7}$$

We will now explain every parameter used in the above set of boundary conditions. The pressure p_0 is just a background pressure on the whole system, a possible choice for this pressure is $p_0 = 0$. The Δp_T is an (extra) applied pressure on the inlet of A to force a Poiseuille flow in tube A, the Δp_I an applied pressure on e to get a Poiseuille flow in the interstitium I. Instead of an applied pressure we can also define a velocity u_T of the fluid going into A and a velocity u_I of the fluid going into I. Note that these velocities only have a component perpendicular to the boundary. The normal force on the fluid at the boundary is given by f_n.
If we use the pressure Δp_t, we can calculate the pressure needed to get a certain average flow by rewriting the average Poiseuille flow from Eq. (4.16) to:

$$\Delta p_T = -u_{avg} \frac{8\eta \Delta x}{R_T}, \tag{5.8}$$

where $\Delta x = L$ is the length of the tube and R_T is the radius of the tube. If we also want to study whether the reabsorption length of our model corresponds with the length l_c in Eq. (3) of Ref. [17], we can calculate the velocity or pressure that is needed to get $L = l_c$ as below.

[17] Or more specific: sodium pumps, because the pumping of sodium is by far the biggest part of the active pumping of ions.
[18] Note that those two flux terms are the only terms contributing to the flux of the ions.

$$u_{avg}^{in} = \frac{2V_m nL}{R_T \rho_0^{ion}}, \tag{5.9}$$

$$\Delta p_T = \frac{16 V_m \eta L^2}{R_T^3 \rho_0^{ion}}, \tag{5.10}$$

where ρ_0^{ion} is the initial concentration of the ions. Note that this means that if we apply this velocity or pressure as a boundary condition on the system, we should find that $\rho^{ion} \approx 0$ at the end of the tube. A derivation of the above equations can be found in appendix C.
After we solve the *Creeping Flow* module, we solve the *Transport of Diluted Species* module and use the calculated velocity profile as an input for this module. We solve the following set of equations:

$$\begin{aligned} \boldsymbol{J^{ion}} &= -D^{ion}\nabla\rho^{ion} + \boldsymbol{u}\rho^{ion}, \\ \nabla \cdot \boldsymbol{J^{ion}} &= 0. \end{aligned} \tag{5.11}$$

Note that we only solve these equations in domain A and I, because we define a flux through C and we are not interested what happens exactly in domain C. The boundary conditions of this system are:

$$\begin{aligned} &\text{a)} && \text{initial concentration } \rho_0^{ion}, \\ &\text{b)} && \text{a flux according to Eq. (3.10) } J_b^{ion} = nV_m \left(\frac{\rho_A^{ion}}{K_m + \rho_A^{ion}} \right)^n, \\ &\text{c)} && \text{a linear extrusion of the flux on boundary b: } J_c^{ion} = \frac{R_T}{R_T + R_C} J_b^{ion}, \\ &\text{d)} && \text{no diffusive flux } \boldsymbol{n} \cdot D^{ion}\nabla\rho^{ion}, \\ &\text{f)} && \text{no diffusive flux } \boldsymbol{n} \cdot D^{ion}\nabla\rho^{ion}, \\ &\text{other boundaries)} && \text{All other boundaries are hard walls with a no-flux boundary condition.} \end{aligned} \tag{5.12}$$

The no-flux boundary condition (on d and f) can be applied because $\boldsymbol{J_{adv}^{ion}} \gg \boldsymbol{J_{dif}^{ion}}$ as shown in Sec. 5.2.1. In Eqs. (5.12) ρ_0^{ion} is the initial concentration, ρ_A^{ion} the concentration in tube A and n the number of ions pumped at the same time. The values for the maximal pumping speed $V_m = 20$ nmol/(cm^{2}s) and the Michaelis constant $K_m = 30$ mmol/L are the same as used in [6, 25]. These values will be used throughout whole this thesis. The scaling factor $R_T/(R_T + R_C)$ is introduced because the surface area between C and I is bigger than between C and A, here R_C is the diameter of the cells (domain C). The normal vector to any boundary is $\boldsymbol{n}$ and D^{ion} is the diffusion coefficient of ions in water.

5.2.4 Results

Below we will discuss the results of the numerical calculations, the values of all relevant parameters can be found in Tab. 3. These values are used in the numerical calculations, unless stated differently.
The numerical solution of Eqs. 5.6 with boundary conditions given by Eqs. 5.7 is a Poiseuille flow. We choose the value of either Δp_T or u_T in a way that we expect to find for the average velocity $u_T^{avg} = 0.6$ mm/s. That means that the solution is given by Eq. 4.14 and the velocity profile looks like Fig. 11. After we find this Poiseuille flow profile we solve the *Transport of Diluted Species module*. We will now show and discuss the results of this calculation.
In Fig. 16 we see the resulting concentration profiles for two different initial concentrations $\rho_0 = 50$ mmol/L and $\rho_0 = 150$ mmol/L. All other relevant parameters have values given by Tab. 3. We also calculate analytically an absolute lower bound for the concentration, by assuming that the ion pumps are pumping at maximum speed irrespective of the ion concentration in the tube. We expect that for high ion concentrations, i.e. $\rho_{ion} \gg K_m$, the numerical and analytical lower bound are approximately the same. In Fig. 16 we see that for the initial value $\rho_{ion} = 150$ mmol/L the numerical solution is, indeed, much closer to the analytical solution than for the initial value of $\rho_{ion} = 50$ mmol/L. We also study whether there are inlet and outlet effects on the concentration profiles, by adding half a tube length at the beginning and end of the tube. This extra length of the tube had no effect on the final results.

Table 3: Values of parameters used in model of the ascending tube

Parameter	Notation	Value
Radius of tube	R_T	10 µm
Diameter of cells	R_C	20 µm
Diameter of interstitium*	R_I	15 µm
Length of tube	L	1 mm
Temperature	T	293.15 K
Viscosity of water**	η	1 mPa·s
Mass density of water	m	998 kg/m^3
Maximal pumping speed	V_m	20 nmol/(cm^{2}s)
Michaelis constant	K_m	30 mmol/L
Number of pumpsites***	n	1
Diffusion coefficient ions	D^{ion}	10^{-9} m^2/s

* Note that the exact diameter of the interstitium is not that relevant for a single tube, because all the physics is independent of R_I. However, for a complete model consisting of 3 tubules the exact value of R_I is significant.
** Viscosity of water at 20 °C.
*** Although $n = 3$ for sodium pumps in human cells [25], we we will use $n = 1$ for simplicity in most of the calculations.

In Fig. 17 we see the different fluxes going in and out of the system as a function of the initial concentration ρ_0. Because we are pumping ions out of tube A with a pumping speed defined by Eq. 3.10, we expect the flux going out of the interstitium I to go asymptotically to a maximum $V = nV_m$. This means that the yellow line in Fig. 17 asymptotically approaches the yellow dashed line, we see that the flux going out of I behaves like this. Note that for the higher concentrations the flux going out of the tube (blue line) is much larger than the flux going out of I (yellow line). This means that only a small amount of the ions is pumped from the tube to I, this is due to the fact that we force the fluid flow that transports the ions through the system to have an average velocity of $u_T^{avg} = 0.6$ mm/s. This fluid velocity is way to high for the pumps to be able to pump almost all the ions from the tube to I. We can also see this in Fig. 16, the concentration at the end of the tube is still about 1/3 of the initial concentration ρ_0 for an initial concentration of $\rho_0 = 150$ mmol/L. Below we will discuss the results of the model is we choose the average velocity of the fluid in such a way that the length of the system L is the same as the characteristic length scale l_c published by Marbach and Bocquet [17].

We will now look at the results where we used different settings for the first step in the calculations. The first step solves Eqs. 5.6 with boundary conditions given by Eqs. 5.7. Above we forced the system to have an average fluid velocity $u_T^{avg} = 0.6$ mm/s. Instead of using this velocity we will now apply a pressure on the system to get $L = l_c$ where L is the length of the tube and l_c the length scale of reabsorption as calculated by Marbach and Bocquet (Eq. (3) of Ref. [17]). The pressure Δp_T that is needed can be calculates using Eq. (5.10). All relevant parameters to calculate this Δp_T can be found in Tab. 3. We again find a Poiseuille flow (qualitatively similar to that in Fig. 11) and after this we solve the *Transport of Diluted Species module*. In Fig. 18 we see the resulting concentration profiles at two different positions in the tube $r = 0$ and $r = 0.9 \cdot R_T$ for an initial concentration of $\rho_0 = 900$ mmol/L. We see that after a length l_c, indeed, the biggest part of the ions is reabsorbed. In the inset of Fig. 18 we can also see that the differences in the ion concentration at different radial positions r are negligible compared to the ion concentration.

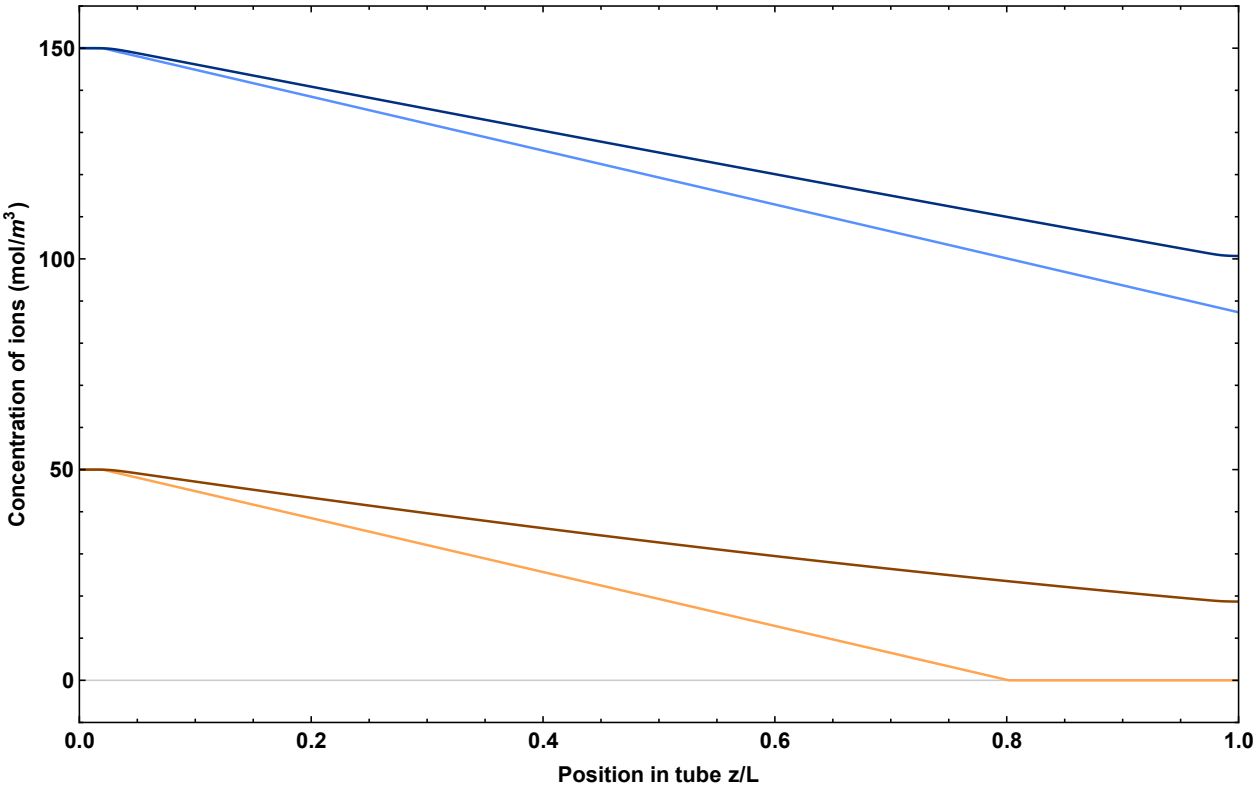

Figure 16: Concentration profiles of ions in the ascending tube of length $L = 1$ mm and radius $R_T = 10$ µm with an initial concentration at the inlet of the tube of $\rho_0 = 150$ mmol/L (dark blue) and $\rho_0 = 50$ mmol/L (dark yellow). The ions are transported through the tube by a Poiseuille flow with an average velocity $u_{avg} = 0.6$ mm/s and are pumped out of the tube by pumps that are described by the Michaelis-Menten kinetics as described in Sec. 3. An absolute lower bound is calculated analytically assuming maximum pumping speed $V = nV_m$ and is plotted for both initial concentrations $\rho_0 = 150$ mmol/L (light blue) and $\rho_0 = 50$ mmol/L (light yellow).

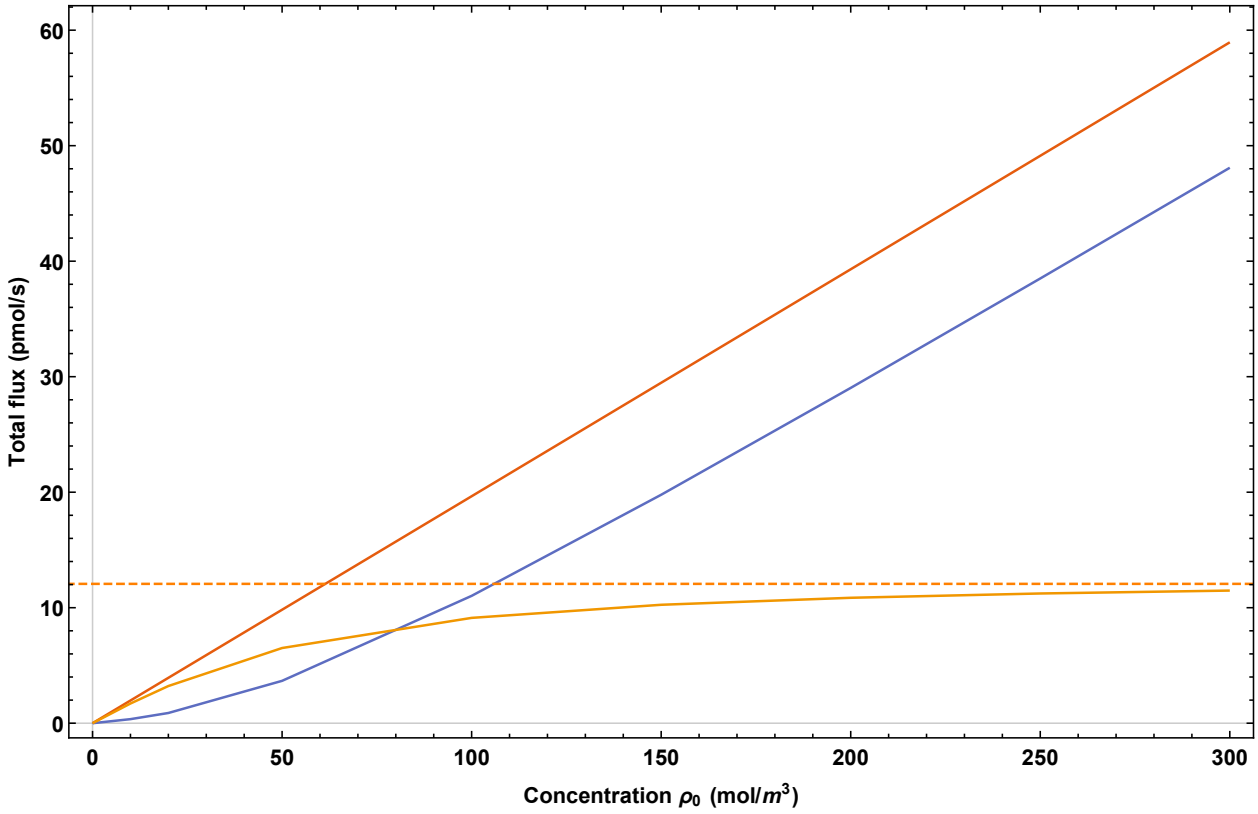

Figure 17: Fluxes going in and out the ascending tube of length $L = 1$ mm and radius $R_T = 10$ μm as a function of the initial concentration ρ_0. Again, the ions are transported through the tube by a Poiseuille flow with an average velocity $u_{avg} = 0.6$ mm/s and are pumped out of the tube by pumps that are described by the Michaelis-Menten kinetics as described in Sec. 3. The flux going into the (orange), the flux going out of the tube (blue) and the flux going out of the interstitium (yellow) are plotted as well as an upper bound for the flux going out of the interstitium (yellow dashed). Note that the flux going out of the interstitium asymptotically goes to this upper bound.

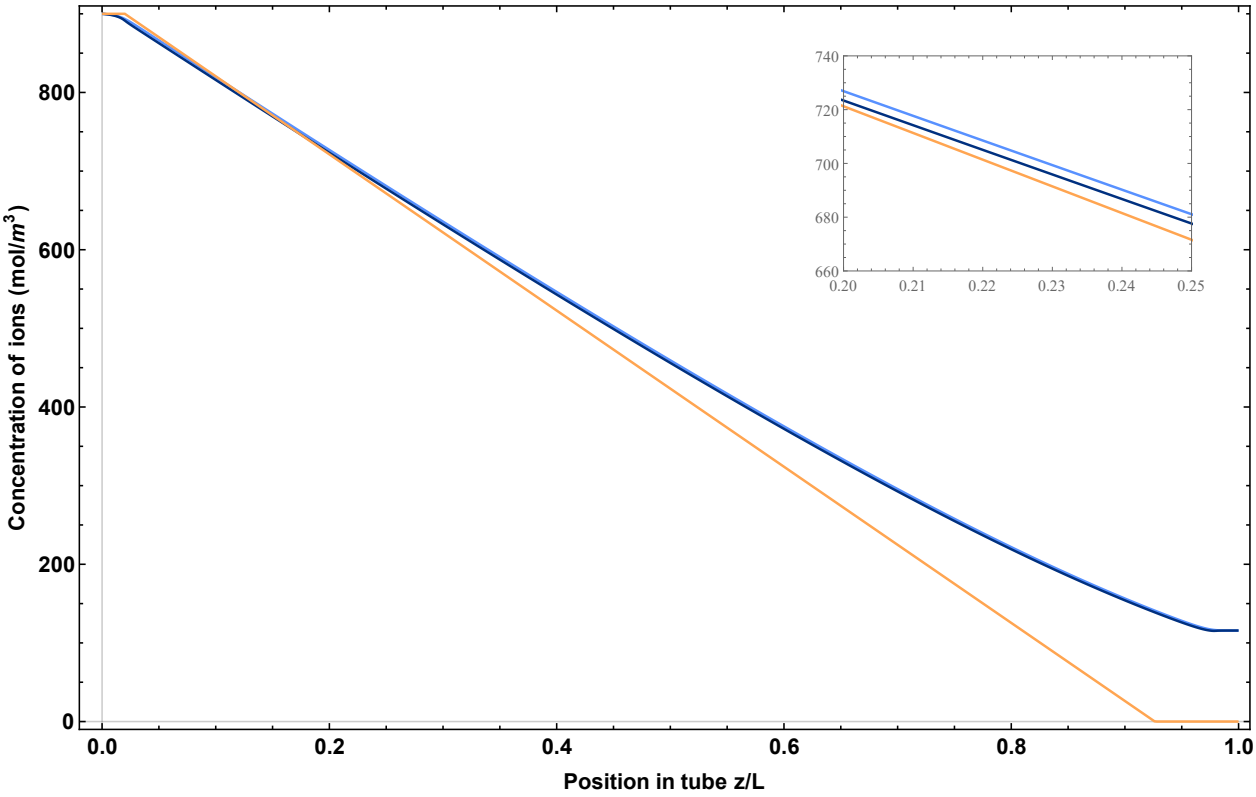

Figure 18: Concentration profiles of ions in the ascending tube of length $L = 1$ mm and radius $R_T = 10$ µm at two different positions $r = 0$ (light blue) and $r = 0.9 \cdot R_T$ (dark blue). The initial ion concentration is $\rho_0 = 900$ mmol/L and the ions are pumped out of the tube by pumps that are described by the Michaelis-Menten kinetics as described in Sec. 3. The applied pressure Δp_T is chosen such that $L = l_c$, where l_c is the length scale of reabsorption as calculated by Marbach and Bocquet (Eq. (3) of Ref. [17]). An absolute lower bound is calculated analytically assuming maximum pumping speed $V = nV_m$ and is plotted (yellow) for the same values of all other parameters. Note that at different positions ($r = 0$ and $r = 0.9 \cdot R_T$) perpendicular to the symmetry axis the concentrations are almost equal due to fast diffusion in this direction.

6 Conclusion, Discussion and Outlook

6.1 Conclusion

We have given a comprehensive description of the kidney in Sec. 2 that can be used as a basis to build a physical model of the kidney. We also built a theoretical physical framework in Sec. 4 and Sec. 3 that one needs to build a physical model of the kidney. With this description of the kidney and the theoretical framework we have tried to build a (numerical) model of the kidney in COMSOL. Unfortunately we were are not able to build a completely working model of the kidney. However, we built some useful building blocks that one can use to build a model of the kidney. The part of the ascending limb is complete and also consistent with the findings of Marbach and Bocquet in [17]. We set up our model in a way that we expect to find that the length of the tube equals the characteristic length of ion reabsorption ($L = l_c$), we find that this is indeed true. However, the way we tried to model the descending limb (and collecting duct) turned out to be non-optimal. This is because using a porous media domain in the model, results in a small flux of ions from the descending tube to the interstitium, that should not be present. So we can conclude that one has to incorporate the semi-permeable wall of these tubes in another way than we did, in the discussion below we will give a suggestion. Our (short) attempt for the connection of the different tubes has not been successful. Partly due to the fact that the flux of ions going in and out of the first tube (descending tube) was not the same, because our model of the semi-permeable wall is not correct. The other reason why the connection of the tubes was not successful will be discussed below.

6.2 Discussion

We are able to build a model of the ascending limb that is consistent with the model published by Marbach and Bocquet [17]. The results of this model and a short discussion can be found in 5.2.4. However, our attempt to build a correct model for the descending limb did not succeed, nor has our attempt for the connection of the different tubes. Below we will discuss the problems we have encountered and give some suggestions to improve the model.

One of the main issues is that we were not able to build a proper numerical model for the descending limb. In other words, we could not make a model in COMSOL that consists of a tube with a wall that is permeable to water and impermeable to solutes, where the solutes are transported by the water (i.e. the solute flux is mostly due to advection). A typical plot of the streamlines of the resulting flow of the model described in Sec. 5.1 can be found in Fig. 19. The problem with this result is that we do not expect a (significant) flow in the longitudinal direction in the cells (domain C). And even worse, we found that the flux of ions from the tube (domain D) to the cells (domain C) is greater than zero. But the wall is defined to be impermeable to the ions. Apparently this is not the way to go to model the descending limb in COMSOL.

We thought about a solution to this problem, but did not have the time to implement it in our model. It might be better to approach the descending limb in the same way as the ascending limb, i.e. by not concerning what happens in the cells lining the tube, but only solve the equations in the tube and in the interstitium. One way this could be done is by using the Starling equation to define a flux (boundary condition) of water out of the tube and after that project this flux to the other side of the cells (boundary between C and I). The Starling equation (obtained from: `https://en.wikipedia.org/wiki/Starling_equation`)[20] :

$$J^{water} = L_p S((p_{H,T} - p_{H,I}) - \sigma(p_{O,T} - p_{O,I})), \tag{6.1}$$

where S is the surface area of filtration, $p_{H,T}$ and $p_{H,I}$ are the hydrostatic pressure in the tube and the interstitium, respectively, $p_{O,T}$ and $p_{O,I}$ the osmotic pressure in the tube and the interstitium, respectively, and σ the Staverman's reflection coefficient (dimensionless). Because it is not our aim to study how the water flows in this region, this may be a good alternative. We thought it was the best way to use a permeable region in our model, but apparently it is not the case. This is possibly because it is a lot more difficult (for COMSOL) to numerically solve the equations for a permeable region than a simple flux condition. If you use this flux boundary condition described above you can also define an osmotic pressure term on the wall

[20] You have to change the definition of the hydraulic conductivity (P_f) from $P_f \to P_f/Pa$ to get the right units (of flux). Compare the factor in front of the pressure difference in the third line of Eq. (1) in [6] with the definition in the above link.

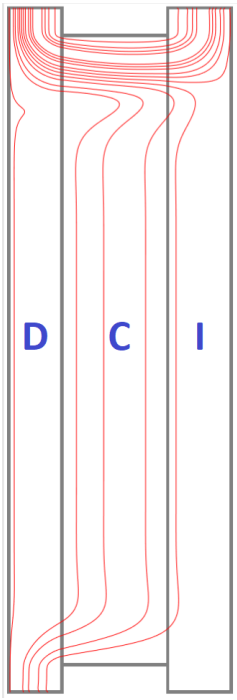

Figure 19: Typical plot of streamlines of the fluid using the model as described in Sec. 5.1

between the cells and the interstitium (boundary between C and I in Fig. 19). Before, this was not possible (in COMSOL you can't define a pressure on a internal boundary).
If one succeeds in building a model of the descending tube one of the problems for the connection of the tubes is solved, but there is still one issue with the connection of the tubes. We used a 2D-axisymmetric geometry where every tube has "his own interstitium", but we want the interstitium that is around each tube to be the same (or at least connected in a correct way). To avoid this problem one could build a fully 3D-model, but this will increase the computation time drastically and therefore is not preferred. Instead of each tube having "his own interstitium" it might be better to treat the interstitium as a separate (extra) tube in which all other tubes can dump fluid or ions. If you use a separate tube for the interstitium you have to think carefully about how and where the fluid an ions enters the interstitium. In COMSOL you can project a flux boundary condition on a tube (e.g. the ascending limb) to a boundary of the interstitium using a *linear extrusion* (or *general extrusion*) operator.
The last problem we will discuss is the fact that we were not sure about how to incorporate the osmotic pressure p_O. As a first attempt we used the van 't Hoff law:

$$p_O = i\rho^{ion}RT, \tag{6.2}$$

where i is the van 't Hoff index (dimensionless), ρ^{ion} the molar concentration of the ions, R the ideal gas constant and T the temperature. But this definition of the pressure resulted in very high pressures in our system, causing unwanted backflows etc. However, if the permeable region is defined in the way described above this may be solved, because in this way there is more freedom to define pressures on boundaries. The osmotic pressure is important to include in the model, because osmosis is the driving force of the (passive) water transport from the tubes to the interstitium.

6.3 Outlook

The most favorable case is that, using the theoretical framework and numerical building blocks we provide in this thesis, one could build a complete model for a filtration device. There are still a few challenges in building a complete model. Most important is the development of a numerical model for a tube with a wall that is permeable to water, but not to the solutes. In the discussion we already provided some ideas for the development of this building block for the model. After that there is the challenge of linking the different

tubes together and dumping the reabsorbed substances in the same interstitium. If these building blocks are made and connected to form a complete model, this model can be used to do numerical calculations on a small filtration devices with a geometry similar to the human nephron. These calculations may be used for the development of water filtration devices or maybe even an artificial kidney.

7 Acknowledgements

I would first like to thank my supervisor Prof. Ren van Roij of the Institute for Theoretical Physics at Utrecht University. The enthusiasm of Prof. van Roij about this topic was a driving force during my research. He consistently allowed this thesis to be my own work, but also provided guidance whenever I needed it.
I would also like to thank Ben Werkhoven MSc for having an open door policy and taking the time to think about problems I ran into. As well as Dr. Joost de Graaf for his expertise and help with the COMSOL sofware.
Finally, I must express my gratitude to my parents and my girlfriend for providing me with unfailing support and continuous encouragement throughout my years of study and through the process of researching and writing this thesis. Thank you.

Author
Johan Verheij

A Derivation of continuity equation

In this section we will derive the continuity equation in 3 dimensions. Consider an infinitesimal volume element as in figure 20 of volume $dxdydz$ and an arbitrary fluid flow. We will write down the mass flux through every surface of this volume and thereafter set the difference between the total mass flux into and out of the volume equal to the total change of mass in the volume. Because the volume element is infinitesimal small the derivative of the flux $\partial \rho v_a / \partial a$ is a constant over the distance da. The mass fluxes through every surface of the volume are

$$1)\rho v_x \qquad 2)\rho v_x + \frac{\partial \rho v_x}{\partial x} dx \qquad 3)\rho v_y \qquad 4)\rho v_y + \frac{\partial \rho v_y}{\partial y} dy \qquad 5)\rho v_z \qquad 6)\rho v_z + \frac{\partial \rho v_z}{\partial z} dz,$$

where ρ is the density of the fluid and v_i the components of the velocity of the fluid.

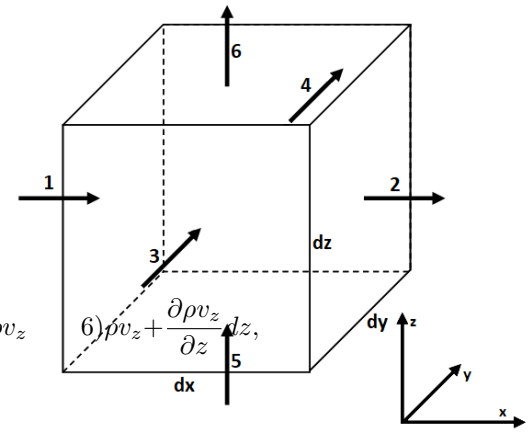

Figure 20: Infinitesimal volume element, the arrows represent mass fluxes in and out this volume element.

The total mass flux in and out of the volume are

$$m_{in} = \rho v_x dydz + \rho v_y dxdz + \rho v_z dxdy$$

$$m_{out} = \left(\rho v_x + \frac{\partial \rho v_x}{\partial x} dx\right) dydz + \left(\rho v_y + \frac{\partial \rho v_y}{\partial y} dy\right) dxdz + \left(\rho v_z + \frac{\partial \rho v_z}{\partial z} dz\right) dxdy.$$

Because the difference between the mass that flows into the volume and out of the volume needs to be equal to the change of the density in the volume this results in

$$\begin{aligned} \frac{\partial \rho}{\partial t} dxdydz &= m_{in} - m_{out} \\ &= \rho v_x dydz + \rho v_y dxdz + \rho v_z dxdy - \left(\rho v_x + \frac{\partial \rho v_x}{\partial x} dx\right) dydz - \left(\rho v_y + \frac{\partial \rho v_y}{\partial y} dy\right) dxdz \\ &\quad - \left(\rho v_z + \frac{\partial \rho v_z}{\partial z} dz\right) dxdy. \end{aligned}$$

Dividing both sides by $dxdydz$ and collecting terms gives

$$\begin{aligned} \frac{\partial \rho}{\partial t} &= \frac{\rho v_x}{dx} + \frac{\rho v_y}{dy} + \frac{\rho v_z}{dz} - \left(\frac{\rho v_x}{dx} + \frac{\partial \rho v_x}{\partial x}\right) - \left(\frac{\rho v_y}{dy} + \frac{\partial \rho v_y}{\partial y}\right) - \left(\frac{\rho v_z}{dz} + \frac{\partial \rho v_z}{\partial z}\right), \\ &= -\frac{\partial \rho v_x}{\partial x} - \frac{\partial \rho v_y}{\partial y} - \frac{\partial \rho v_z}{\partial z}. \end{aligned}$$

Using the definition of the gradient and the definition of flux gives us the desired result

$$\frac{\partial \rho}{\partial t} + \nabla \cdot \boldsymbol{J} = 0.$$

B Fick's law

In this section we will derive Fick's law. If we have a system with many gas particles (e.g. water vapour) that have a kinetic energy, i.e. the temperature $T > 0$, these particles have a kinetic energy. Due to this kinetic energy the particles will move around and collide with each other. Because the particles typically collide every few nanoseconds and because there is no preference direction of this collision, the trajectory of a particle can be seen as a random walk.
Consider a system of particles performing random walks in 1 dimension with typical length scale dx and time scale dt and a volume element dx as in figure 21. Let $N(x,t)$ be the number of particles at position x and time t. At a timestep dt half of the particles at x will move to the right and half of the particles at $x+dx$ will move to the left. So the number of particle moving to the right at 1 and to the left at 2 are

$$1)\ \frac{1}{2}N(x,t) \qquad 2)\ \frac{1}{2}N(x+dx,t).$$

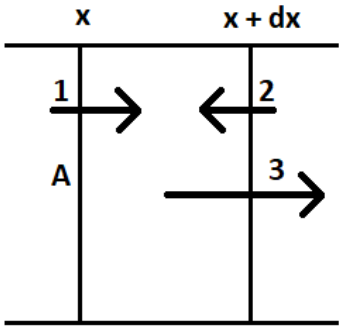

Figure 21: Infinitesimal volume element, the arrows represent particle fluxes in and out this volume element.

So the total particle movement to the right in a volume element dx a time step dt is

$$-\frac{1}{2}(N(x+dx,t)-N(x,t)).$$

The flux J is defined as the net particle movement per area A per time and thus

$$\begin{aligned} J &= -\frac{1}{2}\left(\frac{N(x+dx,t)-N(x,t)}{Adt}\right) \\ &= -\frac{dx^2}{2dt}\left(\frac{N(x+dx,t)-N(x,t)}{Adx^2}\right). \end{aligned}$$

The density is defined as $\rho(x,t) = N(x,t)/Adx$ and we can rewrite the equation above as

$$\begin{aligned} J &= -\frac{dx^2}{2dt}\left(\frac{\rho(x+dx,t)-\rho(x,t)}{dx}\right) \\ &= -D\left(\frac{\rho(x+dx,t)-\rho(x,t)}{dx}\right), \end{aligned}$$

where we defined the diffusion constant in 1 dimension $D = dx^2/2dt$. Now if we take the limit of infinitesimal small dx, the term in parentheses is by definition the derivative of the density with respect to x and this gives us

$$J = -D\frac{\partial\rho(x,t)}{\partial x}.$$

This can be generalized to 3 dimensions and this gives us the desired result

$$\boldsymbol{J(r,t)} = -D\nabla\rho(\boldsymbol{r},t)$$

NB the diffusion constant is dependent on the type of particles.

C Boundary conditions for tube A

We will give a short derivation of Eqs. (5.9) and (5.10) that are used in the model description. These two boundary conditions are chosen such that $L = l_c$, where L is the length of the tube and l_c is the reabsorption length from Eq. (3) as calculated by Marbach and Bocquet [17]. We start from the definition given by Marbach and Bocquet:

$$l_c = \frac{J_{in}^{ion}}{2\pi R_t V_m n}, \tag{C.1}$$

where R_t is the radius of the tube and V_m and n are parameters from the Michaelis-Menten kinetics as defined in Sec. 3. J_{in}^{ion} is the ingoing flux of ions, this flux can be calculated as follows:

$$J_{in}^{ion} = \pi R_t^2 u_{avg}^{in} \rho_0^{ion}, \tag{C.2}$$

where u_{avg}^{in} is the average flow velocity of the ingoing flow and ρ_0 the initial ion concentration. Plugging this definition of J_{in}^{ion} in Eq. (C.1) and setting l_c equal to L we obtain:

$$L = \frac{\pi R_t^2 u_{avg}^{in} \rho_0^{ion}}{2\pi R t V_m n}, \tag{C.3}$$

rewritting this to an expression for u_{avg}^{in} gives

$$u_{avg}^{in} = \frac{2\pi R_t V_m n L}{\pi R_t^2 \rho_0^{ion}},$$

$$u_{avg}^{in} = \frac{2 V_m n L}{R_t \rho_0^{ion}}. \tag{C.4}$$

We see that Eq. (C.4) and the velocity boundary condition in Eq. (5.9) are identical.
For the pressure boundary condition we start from Eq. (C.3) and use that the average flow in the tube is given by the average Poiseuille flow as in Eq. (4.16).

$$L = \frac{R_t \rho_0^{ion}}{2 V_m n} \left(\frac{R_t^2}{8\eta} \frac{\Delta p}{L} \right),$$

rewritting this to an expression for Δp gives

$$\Delta p = \frac{2 V_m n L}{R_t \rho_0^{ion}} \frac{8\eta L}{R_t^2},$$

$$\Delta p = \frac{16 V_m n \eta L^2}{R_t^3 \rho_0^{ion}}. \tag{C.5}$$

We see that Eq. (C.5) and the pressure boundary condition in Eq. (5.10) are identical.

References

[1] M. Elimelech and W. A. Phillip, Science **333**, 712 (2011).

[2] S. G. J. Z. M. P. Peter Scales, Adrian Knight and K. Northcott, *Demonstration of robust water recycling: Energy Use and Comparison* (Australian Water Recycling Centre of Excellence, Brisbane, Australia, 2015), ISBN 978-1-922202-52-9.

[3] T. Humplik, J. Lee, S. OHern, B. Fellman, M. Baig, S. Hassan, M. Atieh, F. Rahman, T. Laoui, R. Karnik, et al., Nanotechnology **22** (2011), URL `https://doi.org/10.1088/0957-4484/22/29/292001`.

[4] B. Corry, J Phys Chem B **112**, 1427 (2008).

[5] M. Heiranian, A. B. Farimani, and N. R. Aluru, Nat Commun **6** (2015), URL `https://www.nature.com/articles/ncomms9616`.

[6] S. Marbach and L. Bocquet, *Active osmotic exchanger for efficient nanofiltration inspired by the kidney supplemental material*, URL `https://journals.aps.org/prx/abstract/10.1103/PhysRevX.6.031008#supplemental`.

[7] R. Greger and U. Windhorst, *Comprehensive Human Physiology*, vol. 1 (Springer-Verlag, Berlin, 1996), 1st ed., ISBN 978-3-642-64619-5.

[8] Baxter, *Phoenix X36 Hemodialysis System*, Baxter (2009), URL `https://www.baxter.com/assets/downloads/products_expertise/renal_therapies/Phoenix_X36_Hemodialysis_System.pdf`.

[9] K. Sembulingam and P. Sembulingam, *Essentials of Medical Physiology* (Jaypee Brothers Medical Publishers (P) Ltd, 2012), 6th ed., ISBN 978-93-5025-936-8.

[10] A. C. Guyton and J. E. Hall, *Textbook of Medical Physiology* (Elsevier Inc., 2016), 13th ed., ISBN 978-1-4557-7016-8.

[11] A. T. Layton, V. Vallon, and A. Edwards, Am J Physiol Renal Physiol **311**, 1378 (2016).

[12] A. Weinstein, Am J Physiol Renal Physiol **308**, 1076 (2015).

[13] A. Edwards, Am J Physiol Renal Physiol **298**, 475 (2010).

[14] S. Thomas, Am J Physiol Renal Physiol **284**, 65 (2000).

[15] A. Layton, K. Laghmani, V. Vallon, and A. Edwards, Am J Physiol Renal Physiol **311**, 1217 (2016).

[16] S. Thomas, WIREs Syst Biol Med **1**, 172 (2009).

[17] S. Marbach and L. Bocquet, Phys. Rev. X **6**, 1378 (2016).

[18] O. Wessely, D. Cerqueira, U. Tran, V. Kumar, J. Hassey, and D. Romaker, Pediatr Nephrol **29**, 525 (2014).

[19] B. Glodny, V. Unterholzner, B. Taferner, K. J. Hofmann, P. Rehder, A. Strasak, and J. Petersen, BMC Urol **9** (2009).

[20] J. F. Bertram, R. N. Douglas-Denton, B. Diouf, M. D. Hughson, and W. E. Hoy, Pediatric Nephrology p. 15291533 (2011).

[21] A. Denic, J. Mathew, L. O. Lerman, J. C. Lieske, J. J. Larson, M. P. Alexander, E. Poggio, R. J. Glassock, and A. D. Rule, N Engl J Med pp. 2349–2357 (2017).

[22] K. Hoang, J. C. Tan, G. Derby, K. L. Blouch, M. Masek, I. Ma, K. V. Lemley, and B. D. Myers, Kidney International **64**, 1417 (2003).

[23] B. S. Institution, *BS 350: Basis of Tables Conversion Factors Part 1* (British Standards Institution, 1974), ISBN 0 580 08471 3.

[24] J. P. Briggs and J. Schnermann, Ann. Rev. Physiol. pp. 251–273 (1987).

[25] R. Garay and P. Garrahan, J. Physiol. **231**, 297 (1973).

[26] R. Noske, F. Cornelius, and R. J. Clarke, Biochimica et Biophysica Acta **1797**, 15401545 (2010).

[27] J. Berg, J. Tymoczko, and L. Stryer, *Biochemistry* (W. H. Freeman, 2002), 5th ed., ISBN 0-7167-3051-0.

[28] L. Michaelis and M. L. Menten, Biochem. Z. **49**, 333369 (1913).

[29] R. van Roij, *Soft Condensed Matter Theory* (René van Roij, Utrecht University, 2018), version used in year 2017-2018.

[30] D. Acheson, *Elementary Fluid Dynamics* (Oxford University Press, 1990), ISBN 978-01-9859-679-0, reprinted in 2009.

[31] D. J. Griffiths, *Introduction to Electrodynamics* (Pearson Education Limited, The address, 2014), chap. 2, pp. 66–70,78,79, 4th ed., ISBN 9781292021423.

[32] R. Greger and E. Schlatter, Pflgers Arch **396**, 325 (1983).